

Tailoring the structure of casein micelles through a multifactorial approach to manipulate rennet coagulation properties

Fanny Lazzaro, Antoine Bouchoux, Jared Raynes, Roderick Williams, Lydia Ong, Eric Hanssen, Valérie Lechevalier-Datin, Stéphane Pezennec, Hyun-Jung Cho, Amy Logan, et al.

▶ **To cite this version:**

Fanny Lazzaro, Antoine Bouchoux, Jared Raynes, Roderick Williams, Lydia Ong, et al.. Tailoring the structure of casein micelles through a multifactorial approach to manipulate rennet coagulation properties. Food Hydrocolloids, 2020, 101, pp.105414. 10.1016/j.foodhyd.2019.105414 . hal-02373068

HAL Id: hal-02373068

https://institut-agro-rennes-angers.hal.science/hal-02373068

Submitted on 21 Dec 2021

HAL is a multi-disciplinary open access archive for the deposit and dissemination of scientific research documents, whether they are published or not. The documents may come from teaching and research institutions in France or abroad, or from public or private research centers.

L'archive ouverte pluridisciplinaire **HAL**, est destinée au dépôt et à la diffusion de documents scientifiques de niveau recherche, publiés ou non, émanant des établissements d'enseignement et de recherche français ou étrangers, des laboratoires publics ou privés.



Distributed under a Creative Commons Attribution - NonCommercial 4.0 International License

Version of Record: https://www.sciencedirect.com/science/article/pii/S0268005X19314730
Manuscript_1a4fe741d26940d1ab119b1377face2c

Tailoring the structure of casein micelles through a multifactorial approach to manipulate rennet coagulation properties

Fanny Lazzaro[1,2*], Antoine Bouchoux[3], Jared Raynes[4], Roderick Williams[4], Lydia Ong[5,6,7], Eric Hanssen[6], Valérie Lechevalier[1], Stéphane Pezennec[1], Hyun-Jung Cho[8], Amy Logan[4], Sally Gras[5,6,7], Frederic Gaucheron[1]

[1] STLO, Agrocampus Ouest, INRA, 35000, Rennes, France

[2] CNIEL, Paris, France

[3] TBI, Université de Toulouse, CNRS, INRA, INSA, Toulouse, France

[4] CSIRO Agriculture & Food, 671 Sneydes Road, Werribee, Victoria 3030, Australia

[5] Department of Chemical Engineering, The University of Melbourne, Parkville, Victoria 3010, Australia

[6] Advance Microscopy Facility, The Bio21 Molecular Science and Biotechnology Institute, The University of Melbourne, Parkville, Victoria 3010, Australia

[7] The ARC Dairy Innovation Hub, The University of Melbourne, Parkville, Victoria, 3110

[8] Biological Optical Microscopy Platform, University of Melbourne, Parkville VIC 3010, Australia

* Corresponding author. STLO, Agrocampus Ouest, INRA, 65 rue de Saint-Brieuc 35000, Rennes, France. flazzaro@hotmail.fr

© 2019 published by Elsevier. This manuscript is made available under the CC BY NC user license
https://creativecommons.org/licenses/by-nc/4.0/

Abstract:

The properties of casein micelles are known to be affected by modifications to the environment, such as variations in pH or the addition of salts, yet the scientific literature typically considers the effects of one factor at a time, while in industrial processes, several modifications are performed simultaneously. The aim of this study was to assess the impact of multifactorial environmental modifications on the colloidal, structural and rennet coagulation properties of casein micelles in a simplified model system. A key finding was that dense regions (~ 20 nm in size) could be released from the casein micelle. The addition of NaCl and $CaCl_2$ had opposing effects, *i.e.* enhancing or limiting this micellar disruption, respectively. A decrease in pH had the strongest impact on the mineral balance, causing the colloidal CaP to solubilize and the micelle to swell. The rennet clotting time was impacted by variations in pH and NaCl content. Interestingly, a consideration of all three levels of casein micelle structure and their interactions was needed to explain variations in the firmness of rennet gels. This study illustrates the complex interplay of factors affecting micellar structure and improves our understanding of how micelles can be manipulated to control their properties.

Keywords: casein micelle, rennet properties, internal structure, multifactorial modifications, small angle neutron scattering, cryo transmission electron microscopy

1 Introduction

In milk, casein proteins (α_{s1}, α_{s2}, β and κ) and minerals (mainly calcium phosphate (CaP) nanoclusters) self-assemble to form a colloid referred to as the casein micelle. Electrostatic, hydrophobic and Van der Waals forces hold the different components together leading to a polydisperse population of particles 100 – 200 nm in diameter (Dalgleish & Corredig, 2012; Holt, Carver, Ecroyd, & Thorn, 2013; Holt, 2016; Holt & Horne, 1996; Horne, 2017; Thorn et al., 2005). There is a consensus that casein micelles are stabilized through electrostatic and steric repulsions due to the presence of a polyelectrolyte brush of κ-casein at the micellar surface (de Kruif, 1999; de Kruif & Zhulina, 1996; Tuinier & de Kruif, 2002). Despite extensive studies the internal structure of the casein micelle, *i.e.* the interactions between caseins and the minerals located within the colloid structure, is still under debate. The recent use of small angle X-ray and neutron scattering (SAXS and SANS, respectively) in parallel with cryo-transmission electron microscopy (cryo-TEM) has enabled questions around the internal structure to be partially answered, although without general agreement (Bouchoux et al., 2015; Bouchoux, Gésan-Guiziou, Pérez, & Cabane, 2010; Day, Raynes, Leis, Liu, & Williams, 2017; De Kruif, 2014; Ingham et al., 2015, 2016; Marchin, Putaux, Pignon, & Léonil, 2007; Pignon et al., 2004; Shukla, Narayanan, & Zanchi, 2009). An early model for the micelle structure was the submicelle model (Schmidt, 1982; Walstra, 1999), more recently a second model has proposed a more open structure composed of dense regions, water channels and CaP nanoclusters.

Environmental factors such as variations in pH, temperature and the addition of salts or chelating agents (de Kort, Minor, Snoeren, van Hooijdonk, & van der Linden, 2011; Gaucheron, 2004; Lazzaro et al., 2017; Silva et al., 2013) induce shifts in the mineral balance between the diffusible and colloidal phases of the casein micelle. These mineral modifications also involve colloidal modifications that lead to changes in the functional properties of the casein micelle, such as the formation and stability of emulsions, thermal stability, and response to acid and rennet coagulation (Broyard & Gaucheron, 2015; Gaucheron, 2004). Although the mineral

fraction only represents a small proportion of the milk components (0.7%), it is used to control the properties of numerous manufactured dairy products.

The response of casein micelles to the addition of chymosin (rennet) and gelation is also of pimary interest. For simplicity, the rennet coagulation mechanism applied to the micelles within many dairy ingredient steams can be divided into three steps: firstly, chymosin hydrolyzes κ-casein located at the surface of the casein micelle by cleaving the Phe(105)-Met(106) bond. Once sufficient κ-casein has been hydrolyzed, depleted micelles aggregate together, as described by many authors including Lucey and colleagues (Lucey, 2002), followed by a reorganization and reticulation to form the casein gel network structure (Dalgleish & Corredig, 2012). In reality this is continual process, and compositional factors such as changes in the fat or protein content (Guinee et al., 1997), pH (Mishra et al., 2005) or the addition of calcium (Udabage et al., 2001) can influence the onset and rate of gelation and the functionality of the resulting gel. Rennet coagulation can be assessed by two main characteristics: (i) the rennet clotting time (RCT), which quantifies the time elapsed from the addition of rennet or chymosin to the detectable onset of gelation, and (ii) the gel firmness. The RCT mainly depends on the rate of the enzymatic reaction and the aggregation of the para-caseinates (first and second steps), while the firmness depends on the organization and the strength of the resulting gel (third step).

Variations in pH and the addition of NaCl and $CaCl_2$ are steps commonly applied to control the coagulation of milk. Many studies have been published describing the separate influence of each of these parameters on the colloidal properties and on the rennet coagulation properties of the casein micelle (Bulca, Wolfschoon-Pombo, & Kulozik, 2016; Choi, Horne, & Lucey, 2007; Daviau, Famelart, Pierre, Goudedranche, & Maubois, 2000; Deeth & Lewis, 2015; Famelart, Le Graet, & Raulot, 1999; Famelart, Lepesant, Gaucheron, Le Graet, & Schuck, 1996; Grufferty & Fox, 1985; Karlsson, Ipsen, & Ardö, 2007; Karlsson et al., 2007; Sandra, Ho, Alexander, & Corredig, 2012; Sbodio, Tercero, Coutaz, & Revelli, 2006; Zhao & Corredig, 2015; Zoon, van

Vliet, & Walstra, 1988, 1989). Although necessary to understand the dissociated effect of each parameter, this monofactorial approach does not correspond to the reality of the dairy industry where a multifactorial approach often occurs with the simultaneous variation of several parameters.

The aim of the current study was to investigate the effect of simultaneous modifications of the physico-chemical parameters on both the colloidal properties and the rennet induced coagulation of casein micelles in a simple model system, with a goal of better understanding the response of casein micelles to environmental changes. An experimental matrix of 27 different suspensions of casein micelles in non-native conditions within water, with variations in added NaCl and $CaCl_2$, at three different pH was designed. A combination of multiple advanced biophysical techniques, such as cryo-TEM and SAXS, was used to make a thorough characterization of the casein micelles in terms of physicochemical, structural and renneting properties. Appropriate statistical analyses were applied to establish the relationships between the colloidal and the rennet coagulation properties of the modified casein micelles, leading to the first study that combines SAXS characterization with an assessment of the functional properties of casein micelles.

2 Materials and methods

2.1 Chemicals

All chemicals used for this study, hydrochloric acid (VWR chemicals, Fontenay-sous-bois, France), NaCl (PanReac AppliChem, Barcelona, Spain), $CaCl_2$ (VWR International, Leuven, Belgium) and sodium azide (Riedek-de Haën, Seelze, Germany) were of analytical grade.

2.2 Materials

Experiments were carried out using a native phosphocaseinate (NPC) powder resuspended in deionised water at 24.2± 0.8 g kg^{-1} of protein. Concentrated NPC was supplied by Gillot SAS (Saint Hilaire de Briouze, France) and obtained by microfiltration (0.1 µm pore size membrane)

of raw skimmed milk followed by diafiltration against milli-Q water. The concentrate was then spray dried according to the method described by Pierre, Fauquant, Le Graet, & Maubois (1992) and Schuck et al., (1994) using Bionov facilities (Rennes, France). Casein and their associated minerals represented more than 90% of the total solid content of the powder. Residual whey proteins (3%) (w/w) and traces of lactose were present in the powder.

For the coagulation experiments, Chr. Hansen (Hoersholm, Denmark) supplied commercial chymosin (CHY-MAX M 200, 200 IMCU ml^{-1}).

2.3 Preparation of casein micelle suspensions

An experimental matrix was designed to assess the concomitant effects of variations in pH and the addition of NaCl or $CaCl_2$. The range of pH and the final concentrations of added NaCl and $CaCl_2$ were selected to produce suspensions which would form gels within one hour after the addition of a set amount of chymosin. The pH values targeted were 5.7, 6.3 or 6.9 and the final concentrations of NaCl and $CaCl_2$ in the suspensions were 0, 50 and 100 mmol kg^{-1} or 0, 7.5 and 15 mmol kg^{-1}, respectively. A full experimental design was carried out, where 27 different suspensions of casein micelles were prepared in water, with different salt and pH environments. The suspensions were named from A to Z, and CTRL to represent the control which consisted of NPC in water at pH 6.9, with no added salts (Fig.1).

Dispersion of the NPC powder in milli-Q water was performed as described in Lazzaro et al., (2017). Briefly, the powder was stirred (900 rpm) at 40 °C for 6 h, followed by an additional 16 h at room temperature overnight. The proper resuspension of the ingredient was checked by laser light diffraction according to Schuck, Dolivet, & Jeantet (2012), ensuring the proportion of insoluble particle was below 10 %. Varying amounts of stock solutions of NaCl (2.5 mol kg^{-1} in milli-Q water, pH 6.9) and $CaCl_2$ (0.25 mol kg^{-1} in milli-Q water, pH 6.9) were added to the concentrated suspensions of NPC in milli-Q water with stirring to reach the required salt concentration. The pH shift induced by the addition of salts was corrected using HCl 1M in milli-Q water and set to 5.7, 6.3 or 6.9. The suspensions were then diluted to 24.2 ± 0.8 g kg^{-1} of

144 protein and left overnight at room temperature. If necessary, the pH was readjusted prior to
145 experiments. For convenience, Tables 1, 2, 3 and Figures 6, 7, 8 report the results of different
146 analyses for a set on 9 samples only. These selected samples correspond to the corners of the
147 cubic experimental design (suspensions A, B, D, E, J, L, M, CTRL ; extreme points) and the
148 center point of the experimental design (suspension T) (Fig. 1).

149 **2.4 Recovery of the diffusible phases of the suspensions**

150 Aliquots (15mL) of each NPC suspension were ultrafiltered by centrifugation for 30 min, at 20°C
151 and 1800 *g*. using Vivaspin concentrators (molecular weight cut-off 10 kDa, Vivascience,
152 Palaiseau, France). The diffusible phases were analyzed to determine the concentrations of
153 diffusible ions and used for the dilution of the suspension for the turbidity (τ) and nanoparticle
154 tracking analysis (NTA) measurements and for the background determination for the SAXS
155 measurements.

156

157 **2.5 Analysis**

158 **2.5.1 Protein content**

159 The total nitrogen content of each suspension was determined according to the Kjeldahl method
160 (IDF standard 20-1, 2014). A factor of 6.38 was used to convert nitrogen to protein
161 concentration. Measurements were performed in duplicate.

162 **2.5.2 Mineral composition and distribution**

163 Total and diffusible cations (calcium Ca, sodium Na) and anions (chloride Cl, inorganic
164 phosphate Pi) contents were determined as described in Lazzaro et al., (2017). Colloidal
165 concentrations were deduced by subtracting the concentration of diffusible ions from the
166 concentration of total ions. The mineral concentrations were adjusted to account for the small
167 differences in protein content (see section 2.5.1.).

168 **2.5.3 Turbidity measurements**

Absorbance measurements were carried out at 600 nm and 20 °C using a UV-visible spectrometer (UVmc², Safas, Monaco).The casein micelle suspensions were diluted 10 times in their diffusible phases and analyzed immediately. The diffusible phase for each suspensions was also analyzed. Absorbance measurements were converted into turbidity (τ) according to the following formula:

$$\tau = 2.303 * \frac{OD(600nm)}{l} \quad (1)$$

with $OD(600nm)$ being the optical density of the suspension (difference between the absorbance of the diluted suspension and the absorbance of its diffusible phase) ; and l the light path length ($l = 1\,cm$).

2.5.4 Nanoparticle tracking analysis

Nanoparticle Tracking Analysis (NTA) was performed at 20 °C using a Nanosight NS300 (Malvern Instruments, Malvern, United Kingdom) equipped with a Nanosight syringe pump. The principle of NTA is based on the tracking of individual particles in suspension. A large dilution (40,000 times) of the casein micelle suspension in their own diffusible phase was necessary to meet the optimal settings of the apparatus, *i.e.* 20 – 100 particles per frame during the measurement combined to a dark background image. A syringe was loaded with the diluted suspension and the focus adjusted manually. The infusion rate was set to 20, the camera level to 12 and 5 video images of 60 s each were recorded. The video images of the movement of particles under Brownian motion were analyzed by the NTA image analysis software (V 3.0 0064., Malvern Instruments). The minimum screen gain, and detection threshold of 3 were selected to maximize the detection of small particles (< 50 nm diameter). The particle size distributions obtained (data not shown) were fitted with a log-normal population of particles using Schulz equation (Schulz, 1935):

$$W(R, r_{NTA}, \sigma) = \frac{R^Z}{\Gamma(Z+1)} \left(\frac{Z+1}{r_{NTA}}\right)^{Z+1} \times exp\left[-\frac{R}{r_{NTA}}(Z+1)\right] \quad (2)$$

193 Where r_{NTA} is the average radius of the particles and Z relates to the polydispersity (σ) of the
194 particle radii (R) given by the expression:

195 $$\sigma = \left(\frac{\overline{R^2}}{r_{NTA}} - 1\right) = \frac{1}{Z+1} \quad (3)$$

196 The value of σ varied from 0.23 to 0.47 within the set of suspensions and r_{NTA} was further used
197 in the statistical analyses.

198 **2.5.5 Cryogenic Transmission Electron microscopy**

199 A thin vitrified film of casein micelle suspension was prepared as described in the method of
200 Chen et al., (2011). A Formvar lacey carbon film mounted on a 300 mesh copper grids
201 (ProSciTech, Queensland, Australia) were glow discharged for 15 s and used as a hydrophilic
202 support on which the suspensions (4 µL) were adsorbed. After 30 s, the grids were plunged in
203 liquid ethane using a Vitrobot (FEI Company, Eindhoven, Netherlands) to freeze the sample.
204 The grids were observed on a Technai G2 TF30 (FEI company, Eindhoven, Netherlands)
205 operating at 200 kV and equipped with a Gatan US1000 2kX2k CCD Camera (Gatan). Between
206 10 and 20 micrographs per suspension were recorded under low-dose conditions with defocus
207 values of 4 - 6 µm. Image analysis was performed using Image J software (National Institute of
208 Health, USA). Due to the large numbers of samples, this process was automated through the
209 use of macros set up within Image J. In total, between 1,554 particles (in suspension TEM) and
210 29,092 particles (in suspension B) were measured in three steps:

211 i) The region of interest (ROI) was defined:

212 Particle detection was strictly limited to the area free from the grid structure and ice particles
213 present as a result of sample preparation.

214 ii) Particle detection:

215 To detect particles, the background was subtracted from images using a 'rolling ball' algorithm
216 and smoothed using Gaussian filtering before the threshold was applied and particles measured.
217 Touching particles were separated using the distance transform watershed plugin (Quasi-

Euclidean). Most of the very large particles (diameter > 50 nm) were often partially hidden by the grid. Therefore, the grid-obstructed particles were excluded from the detection only if more than 10% of the area defined by the best-fitted ellipse drawn around the particle was hidden under the grid. In order to prevent any misrepresentative segmentation, which can be caused from automatic detection, all segmentation results were visualized and the overlay was saved as a separate image that was manually inspected.

iii) Shape measurement of the particles:

Feret's diameter was determined for each particle detected. Particles were defined as small (< 50 nm in Feret's diameter) or large (> 50 nm in Feret's diameter). The ratio of small to large particles was then calculated for each suspension and defined as $\Gamma_{s/l}$.

2.5.6 Small angle X ray scattering measurements, data treatment and modelling

The SAXS measurements were carried out on the suspensions and their respective diffusible phases at the SAXS/WAXS beamline of the Australian Synchrotron (Clayton, Melbourne, Australia). The beamline is equipped with a Pilatus 1 M detector (170 mm x 170 mm, effective pixel size of 172 x 172 µm). Each sample was measured at sample-to-detector lengths of 7.106 m and 0.721 m with respective photon energies of 8.2 keV (1.512 Å) or 18.1 keV (0.685 Å). Merging the data from both distances provided a q range of 1.3 x 10^{-3} to 1.93 $Å^{-1}$. The samples were drawn into a 1.5 mm glass capillary; allowing continuous flow through the X-ray beam during measurements. The data were obtained from at least 10 exposures of 2 s intervals at 20°C. The capillary was rinsed with water, followed by 8 M guanidine and again with water before being air-dried between each sample analysis.

The SAXS intensities were normalized to an absolute scale and at least 10 measurements per sample were averaged to obtain the intensity profiles using ScatterBrain (V 2.71) (Australian Synchrotron, Clayton, Australia). Measurements of the diffusible phases for each suspension were subtracted from the corresponding scattering intensities of the suspensions to account for background. Finally, the intensities were adjusted to account for the difference in total protein

content of the suspensions in Primus (V 3.2) (ATSAS, Hamburg, Germany). Igor software (V 7.0.2.2) (Wave Metrics, Lake Oswego, USA) was used to merge the data from the 7.106 and 0.721 m detector distances to obtain the final curves I = f(q).

The SAXS scattering intensity curves were fitted according to the model of Bouchoux et al., (2010) with slight modifications. This model considers three populations of particles: Population A, observed at low q (up to 6 x 10^{-3} $Å^{-1}$) where the scattering intensity corresponds to the presence of casein micelles; population B, in the intermediate q regions (6 x 10^{-3} to 2 x 10^{-2} $Å^{-1}$), where the scattering corresponds to dense regions inside the casein micelles and population C; at high q (7-8 x 10^{-2} $Å^{-1}$) attributable to the CaP nanoclusters. The intensity depends on the form factor of each population $P_n(q)$ (approximated by the form factor of polydisperse spheres of mean radius r_a, r_b and r_c) and on prefactors a, b and c:

$$I(q) = a\,P_a(q) + b\,P_b(q) + c\,P_c(q) \quad (4)$$

with:

$$a = \alpha \times n_a\,(Vma\ \times\ \Delta\rho_a)^2 \quad (5)$$

$$b = \alpha \times n_b\,(Vmb\ \times\ \Delta\rho_b)^2 \quad (6)$$

$$c = \alpha \times n_c\,(Vmc\ \times\ \Delta\rho_c)^2 \quad (7)$$

where n_a, n_b, n_c were the number of scatterers for each population, Vma, Vmb, Vmc their volume and $\Delta\rho_a$, $\Delta\rho_b$, $\Delta\rho_c$ their contrast, respectively.

The absolute number of casein micelles was assumed to be the same in all the suspensions. This hypothesis is based on the observations of Moitzi, Menzel, Schurtenberger, & Stradner, (2011) that a decrease in pH left the number of casein micelles unmodified, even if some casein micelle materials are subdivided into individual monomers or smaller casein aggregates with a resulting decrease in micelle size and mass. In the present study, it was also assumed that the modifications of the pH and the addition of NaCl and $CaCl_2$ applied in the experimental design were not sufficient to cause the complete disruption of the micellar structure. This implies that the n_a value is not affected by the physical-chemical modifications of our samples. We chose to

set it n_a to 1 so that n_b and n_c are defined relative to a singular casein micelle. As a consequence, the constant α accounts for both the electron scattering length and the absolute number density of casein micelles in the samples.

This model was tested on our data according to the procedure of Bouchoux et al., (2010). First, the value of the radius of each population, r_a, r_b and r_c, and the prefactors, a, b, c, were determined by fitting the model to the experimental data with polydispersities set to $\sigma_a = 1/3$, $\sigma_b = 1/3$ and $\sigma_c = 0.2$. The good quality of the fits support the value of polydispersity used in this study to describe scattering that relates to casein micelle size. Note that we decided not to use the polydispersity values determined by NTA (2.5.4) given that the SAXS and the NTA methods cover different size ranges for the assessment of the physical properties of the particles in suspension.

In a second step, the value of the constant α was calculated from the control sample (CTRL) using the prefactor a obtained from the fit, the size (and therefore volume) of the micelle in this case, and the contrast $\Delta\rho_a$ of a native casein micelle in water, *i.e.* 0.018 e- $Å^{-3}$ (ρ_{water} = 0.334 e- $Å^{-3}$ and $\rho_{caseinmicelle}$ = 0.352 e- $Å^{-3}$).

In a third step, the values of $\Delta\rho_a$, n_b and n_c were calculated for the 27 suspensions using the sizes and prefactors obtained from the fits. The micelle, $\Delta\rho_a$ was simply calculated from prefactors a and sizes r_a, knowing that n_a = 1. The number of dense regions n_b was calculated from prefactors b, sizes r_b, and making the assumption that contrast $\Delta\rho_b$ is relatively insensitive to the physical-chemical modifications performed in this study. $\Delta\rho_b$ is taken as 0.035 e- $Å^{-3}$, *i.e.* twice the contrast of the micelle assuming that dense regions occupy 50% of the total volume of the casein micelle (Bouchoux et al. 2010). The CaP nanoclusters / Protein inhomogeneities, n_c was calculated from prefactors c, sizes r_c, and an estimated contrast $\Delta\rho_c$ of 0.172 e- $Å^{-3}$ that was also assumed to be constant between samples. Note that in a recent work, Ingham et al., (2016) suggest a new interpretation and assign the high q features of SAXS data to the presence of inhomogeneous protein structures of 1-3 nm length scale instead of CaP nanoclusters. As our

296 purpose is not to take a position on this question, we decided not to restrict our analysis solely to
297 the interpretation of Bouchoux et al. (2010). A number of possible inhomogeneities n_{cPI} was
298 therefore calculated following Ingham's postulate, this time using an estimated contrast of 0.126
299 e- $Å^{-3}$ (Ingham et al., 2016).

300 **2.5.7 Rennet coagulation properties**

301 The coagulation properties of samples were assessed using a ChymoGRAPH® (Chr Hansen,
302 Denmark) which uses a similar physical principal to the Formagraph (McMahon & Brown, 1982)
303 and where coagulation is determined according to the movement of a stainless steel, loop
304 pendulum immersed in the samples. Casein micelles suspensions (10 g) were weighed into the
305 wells of the ChymoGRAPH® stainless steel block which was immersed in a water bath for 10
306 min to equilibrate the temperature of the block and suspension to 30°C. A sample of 400 µL of
307 the enzyme solution (chymosin diluted ten times in milli-Q water) was added and the
308 suspensions, stirred for 30 s with the spoons and transferred from the water bath to the
309 oscillating plate. A Peltier module maintained the temperature of the block at 30°C. When the
310 coagulation began, the resulting increase in viscosity and the formation of gels caused the
311 pendulums to oscillate together with the samples. The movement of each pendulum was
312 measured by the use of optical fibers over a period of 60 min and the data collected using the
313 ChymoGRAPH® software (V 1.0, Chr Hansen, Denmark). The RCT corresponded to the time
314 elapsed from chymosin addition to the detectable onset of gelation, where gelation was defined
315 as at the time point when the firmness of the suspensions was > 0. The maximal firmness
316 recorded during the 60 min duration of the experiment was defined as the firmness of the gel.

317 **2.5.8 Statistical treatments**

318 As mentioned in section 2.3., a complete experimental design was carried out to study the
319 combined effects of variation in pH (5.7, 6.3, 6.9), NaCl addition (0, 50, 100 mmol kg^{-1}) and
320 $CaCl_2$ addition (0, 7.5, 15 mmol kg^{-1}) on the colloidal and renneting properties of the casein
321 micelles (Fig. 1).

322 The data set was subjected to principal component analysis (PCA) to highlight relationships
323 between measured variables, and similarities between samples. The general purpose of PCA is
324 to summarize a data set with an optimized, controlled loss of information (Jolliffe, 1986; Abdi &
325 Williams, 2010). It allows one to identify patterns which are the most representative of the
326 variability in the whole data set, and to locate individual samples on similarity maps based on
327 these patterns.
328 If the data consist in p variables measured for each of the samples, any sample may be
329 represented as a point in a p-dimensional space. Then, PCA can be viewed as the projection of
330 the data on a subspace which maximizes the dispersion of the projected data (variance
331 maximization). The axes that define this subspace, are new variables, called principal
332 components, which are linear combinations of the p initial variables. They are orthogonal (thus
333 uncorrelated) and ordered by decreasing projected variance, in such a way that the few first
334 principal components account together for the most part of the variability (the "information") in
335 the data set. For each principal component, the coefficients for the p initial variables (called
336 "loadings") illustrate their respective contributions in the principal component, and are used to
337 interpret the physical meaning of the new variable. Each sample is then characterized by the
338 respective values taken by these new variables, called the scores of the sample on the different
339 principal components. These scores represent the coordinates of each sample on a factorial
340 map, whose axes origin corresponds to the average spectrum.
341 PCA was performed after variable centering and scaling to unit variance using the R software
342 package (R Core Team, 2018) and the FactoMineR package (Lê, Josse, & Husson, 2008). All
343 the correlations mentioned in the results and discussion section were found to be significant ($p <$
344 0.05) using the paired student t-test.
345 In addition, multiple linear regression was also applied to the SAXS variables r_a, n_b and n_{cCaP},
346 using the software STATGRAPHICS Centurion XVII (V. 17.1.10, Statpoint Technologies, The
347 Plains, USA) in order to evaluate the effect of these structural features on the firmness of the

gel. A model of firmness was defined that included the quadratic effects of r_a, n_b and n_{cCaP} and the second order interactions between these factors. The full equation of the model was:

$$Firmness = constant + r_a + n_b + n_c + r_a^2 + n_b^2 + n_c^2 + (r_a \times n_b) + (r_a \times n_c) + (n_b \times n_c) \quad (8)$$

The LS-means were calculated and differences regarded as significant for $p < 0.05$. Non-significant effects were excluded from the model, except when first order effects were participating in interaction effects.

3 Results and discussion

The experimental protocol applied in this study allowed the effect of variations in added NaCl and $CaCl_2$ on the colloidal properties and gelation properties of the casein micelle to be examined. Analysis was performed at three different pH, and conditions for each suspension were non-native and carefully controlled, to allow for compositional structure-function effects to be isolated.

The results of the biophysical analyses are presented and discussed in two main sections. In the first section, the PCA analyses are used to (i) assess the impacts of variation in pH and the addition of NaCl and $CaCl_2$ on the mineral balance of the casein micelle, (ii) establish relationships between the structure of the casein micelle and its other colloidal properties. In the second section, the relationships between rennet coagulation properties and colloidal and structural features of casein micelle are considered. For these experiments rennet is added to induce coagulation, but no starter culture is added to simplify the model experimental system examined. PCA analyses were able to explain the variation observed in RCT, while linear regression is able to explain interactions between the structural properties and the firmness of the rennet gels.

3.1 Colloidal and structural properties of the modified casein micelles

373 In the general case, the output of PCA is dual: it consists numerically in i) the loadings of the
374 initial variables in each of the principal components, which illustrate the main dimensions of
375 variability in the data set, and ii) the scores of the samples on the principal components, *i.e.* their
376 coordinates on similarity maps.
377 It was found that almost 80 % of the variability (total variance) observed within our experimental
378 design is accounted for together by the first four principal components (34.4 %, 23.5 %, 11.2 %
379 and 10.1 %, respectively). To illustrate the respective contributions of the initial variables to
380 principal components, one may use correlations between initial variables and principal
381 components, *e.g.* as in Fig. 2 and Fig. 4.
382 As a rule of interpretation and for example, PC1 is highly positively correlated with colloidal Ca,
383 while PC2 is highly positively correlated with diffusible Na (Fig. 2). Any sample with a high
384 positive score on PC1 (PC2, respectively) would then be characterized by a high content in
385 colloidal Ca (diffusible Na, respectively).

386 **3.1.1 Impact of the environmental modifications on the mineral balance of the casein**
387 **micelle**

388 Analysis of the partition of minerals Ca, Pi, Na and Cl between the colloidal and diffusible
389 phases of the suspensions (Table 1) revealed that the colloidal ions consisted mainly in Ca and
390 Pi, whereas Na and Cl were mainly present in the diffusible phases of the suspensions when
391 NaCl was added. Figure 2 shows the strong, positive correlations between the pH and colloidal
392 Ca and Pi (0.85 and 0.80, respectively) and a negative correlation with the concentration of
393 diffusible Pi (- 0.86). The diffusible Ca concentration was weakly, but still significantly, impacted
394 by variation in pH, with a correlation coefficient of - 0.5 (Fig. 3).
395 The strongest variation of Ca in the diffusible phase was attributed to the addition of $CaCl_2$, with
396 a correlation coefficient of 0.84 (Fig. 4). Colloidal and diffusible concentrations of Pi were also
397 significantly impacted by the addition of $CaCl_2$ but to a much smaller extent, with correlation
398 coefficients of 0.42 and - 0.42 respectively (Fig. 3). These results confirm that modifications in

399 pH and $CaCl_2$ induced opposite effects on the mineral content of the casein micelle, with pH
400 inducing a stronger effect compared to $CaCl_2$ addition.
401 A decrease in pH led to the solubilization of the CaP nanoclusters, which has been reported in
402 the literature (Dalgleish & Law, 1989; Daviau, Famelart, Pierre, Goudrdranche, & Maubois,
403 2000; Famelart, Lepesant, Gaucheron, Le Graet, & Schuck, 1996; Le Graet & Brulé, 1993; Le
404 Graet & Gaucheron, 1999; Le Ray et al., 1998; van Hooydonk, Boerrigter, & Hagedoorn, 1986;
405 Zoon, van Vliet, & Walstra, 1989). Conversely, the addition of $CaCl_2$ limited CaP solubilization
406 presumably by shifting the Ca^{2+} equilibrium through the saturation of the diffusible phase (Moitzi
407 et al., 2011). Added Ca would also directly associate with caseins and/or with the diffusible Pi
408 and precipitate as CaP (Le Ray et al., 1998; Philippe, Le Graet, & Gaucheron, 2005; Philippe,
409 Gaucheron, Le Graet, Michel, & Garem, 2003; Udabage, McKinnon, & Augustin, 2000).
410 The addition of NaCl positively correlated with the diffusible Na and Cl concentrations (0.99 and
411 0.95, respectively) (Fig. 2), which was consistent with the presence of NaCl in the diffusible
412 phase. No significant correlation was found between NaCl addition and the concentrations of
413 colloidal ions (Fig. 2) *i.e.* NaCl had no direct effect on the mineral content of the casein micelle
414 within the range studied (0 to 100 mmol kg^{-1}). This result is in agreement with the finding of
415 Karlsson, Ipsen, & Ardö (2007) who reported no change in the colloidal CaP content. However,
416 this observation differs from the results of Aoki, Umeda, & Nakao, (1999); Famelart et al.,
417 (1996); Grufferty & Fox, 1985; Zhao & Corredig, (2015); Zoon et al., (1989) who reported that
418 solubilization of Ca, and occasionally Pi, occurred when NaCl was added to fresh or
419 reconstituted skim milk or casein micelle suspensions. These discrepancies could arise from
420 differences in pH, as in most cases, variations in pH induced by NaCl addition were not
421 corrected, and/or the amount of added NaCl was 3 to 5 times higher than in the present study.
422 **3.1.2 Consequences on the structural properties of the casein micelle**
423 The SAXS data presented in Fig. 5 were treated primarily using the sponge-like model defined
424 by Bouchoux, Gésan-Guiziou, Pérez, & Cabane, (2010) which uses three populations to

interpret the SAXS pattern of casein micelles. The alternate interpretation of Ingham et al., (2016) also defines three population but attributes population C; at high q (7-8 x 10^{-2} $Å^{-1}$), to protein inhomogeneties rather than the CaP nanoclusters. Given that we have decided not to rely exclusively on the interpretation of either Ingham et al., (2016) or Bouchoux et al., (2010), the implications of both studies are discussed here. The SAXS patterns (Fig. 5) show variability in the intensity of signal across these 3 different regions for the set of 9 selected samples. The structural features determined from the SAXS data (r_a, $\Delta\rho_a$, r_b, n_b, r_c, n_c) for the 27 suspensions were compared to the other physico-chemical variables (*e.g.* concentrations of colloidal and diffusible minerals, τ, r_{nano}, $\Gamma_{s/l.}$) for each population of scatterers (A, B and C) and analysed by PCA (Figs. 2, 3, 4). These correlations and the relevance of the two SAXS models applied are discussed in the following sections.

3.1.2.1 Population A: the casein micelle

The modelling of the SAXS data enabled 2 variables, r_a and $\Delta\rho_a$, describing the casein micelle radius and its contrast to be defined, respectively. The radius, r_a varied from 41.5 to 58.1 nm (Table 2), which is consistent with values determined in earlier characterizations of milk or casein micelle dispersions by SAXS (Bouchoux et al., 2010; Ingham et al., 2016; Pignon et al., 2004; Shukla et al., 2009). Moreover, r_a positively correlated with the mean micellar radius measured by NTA, r_{NTA} ($53.8 < r_{NTA} < 74.8$ nm) of the different suspensions (Fig. 2 and Table 2), with a correlation coefficient of 0.72. These size measurements are close to those for native casein micelles in milk measured by NTA (Priyashantha et al. 2019).

The PCA also suggests a dependency between the micellar size and mineral balance. Indeed, r_a showed negative correlations with colloidal concentrations of Ca and Pi (- 0.71 and - 0.38, respectively) and a positive correlation with the concentration of diffusible Pi (0.38) (Fig. 2). The solubilization of the micellar CaP caused by a decrease in pH resulted in an increase in micellar size due to swelling. This size increase also affected the turbidity of the suspensions that increased (correlation coefficient of - 0.46 between pH and τ) (Fig. 2). These results were in

451 agreement with those of Daviau et al., (2000) and van Hooydonk et al., (1986) but differed to the
452 observations of Moitzi et al., (2011) and Ouanezar, Guyomarc'h, & Bouchoux, (2012). These
453 last authors reported a decrease of micellar diameter, measured by multiple angle 3D light
454 scattering or by AFM microscopy, respectively. In these studies, skim milk and casein micelle
455 powders were resuspended in deionised water or synthetic milk ultrafiltrate (lactose free saline
456 solution), respectively, providing a different ionic environment for the casein micelles than in our
457 study. In addition, the pH ranges covered in these studies were lower than herein, possibly
458 leading to differences in behavior when the colloid is exposed to more severe conditions.
459 $CaCl_2$ addition had no impact on r_a (Fig. 3), which was in agreement with results reported by
460 Philippe et al., (2005); Philippe et al., (2003) and Udabage et al., (2000). Conversely, the
461 concentrations of NaCl and diffusible Na significantly correlated with r_a (- 0.46, - 0.43,
462 respectively) (Fig. 2), with NaCl addition slightly reducing the diameter of the casein micelle. This
463 differs from the findings of Zhao & Corredig, (2015) and Karlsson, Ipsen, Schrader, & Ardö,
464 (2005), where an increase in the size of casein micelles was observed. It is possible, however,
465 that in these previous studies, the increase in size was due to the decrease in pH (not corrected)
466 induced by NaCl addition rather than the direct effect of the soluble NaCl salt. Here, τ negatively
467 correlated with NaCl (- 0.46) (Fig. 2), reflecting a decrease in scattering following NaCl addition.
468 This result was in accordance with the two studies cited above and could be caused by a
469 decrease in micellar size and/or internal rearrangements of the micelle structure. Diffusible Na
470 may screen the negative charge on κ-casein CMP, causing a partial collapse of the hairy layer
471 and a slight decrease in micellar size. The impact of NaCl on the size and turbidity of the casein
472 micelles could also be related to the release of small casein aggregates (dense regions) from
473 casein micelles. This argument is developed further in section 3.1.2.2 of the present paper. $\Delta\rho_a$,
474 defined as the contrast of the casein micelle, corresponds to the electron density of the micelle
475 (ρ_{CM}) relative to the electron density of the diffusible phase (ρ_{DF}), which consists of water
476 containing ions (Ca, Na, Cl and Pi) from the NPC powder and/or the addition of NaCl and $CaCl_2$.

The contribution of these diffusible ions to ρ_{DF} ranged from 0.02 to 0.73 %, and thus, was not taken into account here and ρ_{DF} was considered constant and equal to the electron density of water, (0.334 $e^- Å^{-3}$). Therefore, in the present study, $\Delta\rho_a$ directly reflected the variation of the electron density of the casein micelle. This value depended on the volume, the casein concentration and the CaP content of the casein micelles. $\Delta\rho_a$ varied between 0.010 and 0.018 $e^- Å^{-3}$ (Table 2), which is of same order of magnitude as the contrast of a native casein micelle described by Bouchoux et al., (2010) and Ingham et al., (2016). $\Delta\rho_a$ presented a negative correlation (-0.86) with r_a (Fig. 2). It also positively and strongly correlated with concentrations of colloidal Ca and Pi (0.90 and 0.67, respectively) (Fig. 2). These results were consistent with an increase in the volume of the casein micelle due to a depletion in CaP, leading to a decrease in the electron density of the micelle.

3.1.2.2 Population B: the dense regions

The scattering caused by population B is characterized by r_b, the radius, and n_b, the number of dense regions per casein micelle. Both features showed variability within the full sample set, with RSD's of 38.9 and 84.1 %, respectively (Table 2). PCA analysis (Fig 2.) indicates a strong and positive correlation (0.73) between n_b and Γs/l, the ratio of small (< 50 nm in Feret's diameter) to large (> 50 nm in Feret's diameter) particles detected on cryo-TEM micrographs (section 2.5.5) (Fig. 6).

Large black and homogeneous strands crossing the cryo-TEM micrographs (Fig. 6) correspond to the grids that support the suspensions and large circular spots (*e.g.* suspension E) or merged spots (*e.g.* suspension D) were individual casein micelles and aggregates of casein micelles, respectively. Differences in the granularity of the background of the images were attributed to the presence of small-dissociated aggregates of the casein micelle that were present in the diffusible phase. This feature was directly quantified by the ratio $\Gamma_{s/l.}$. Image analysis revealed that these small particles have diameter of around 5 nm (around the resolution limit of the TEM microscope) to 50 nm (data not shown), which was is agreement with the size range of the

503 population B modelled by SAXS measurements (from 6.1 nm to 21.9 nm in radius – Table 2).
504 This correlation between the increase in n_b and $\Gamma_{s/l.}$ suggests that the dense protein regions
505 detected by SAXS were not only present inside the micelle but could also be present outside the
506 casein micelle in the diffusible phase, although the composition of the particles outside the
507 casein micelle is not known.
508 A positive correlation of 0.49 was also observed between n_b and both NaCl and diffusible Na
509 (Fig. 2), indicating that NaCl addition increased n_b. Conversely, enrichment of the suspensions
510 with $CaCl_2$ weakly but significantly, reduced n_b (correlation coefficient of - 0.39) (Fig. 7). Small
511 particles of around 20 nm in diameter were also observed by Müller-Buschbaum, Gebhardt,
512 Roth, Metwalli, & Doster (2007) using atomic force microscopy under similar conditions. These
513 authors reported a decrease of the number of small particles in the presence of increasing Ca,
514 consistent with observations here. To date, only the present study and that of Müller-Buschbaum
515 et al., (2007) report the presence of dissociated aggregates outside of the casein micelle based
516 on observations by microscopy and SAXS. It is reasonable to assume, however, that such small
517 particles would not sediment by ultracentrifugation and a parallel can be established between
518 our observations and the increasing presence of caseins in the supernatant obtained by
519 ultracentrifugation, defined as soluble caseins. Our observations are also consistent with
520 Famelart et al., (1999); Zhao & Corredig, (2015), who reported an increase in the concentration
521 of soluble casein after NaCl addition. Conversely, Famelart et al., (1999); Philippe et al., (2005);
522 Udabage et al., (2000) observed a decrease in soluble caseins when $CaCl_2$ was added. This
523 may be explained by considering the actions of these two ions. NaCl would be responsible for
524 the disruption and loosening of the internal structure of the casein micelle by neutralizing
525 negative charges on the casein chains, whereas $CaCl_2$ would either favor the creation of new
526 bonds between the phosphorylated caseins and/or prevent the dissociation of casein materials
527 by limiting the solubilization of CaP nanoclusters. Our finding of an increase in soluble casein

528 due to pH-induced dissociation of CaP nanoclusters is also consistent with reports by Dalgleish
529 & Law, (1989); Le Graet & Gaucheron, (1999);and van Hooydonk et al., (1986).
530
531 In the present study, there was no significant correlation between pH and n_b (Fig. 2). There was
532 however, a direct and strong effect of pH on n_{cCaP} (the number of population C scatterers per
533 micelle, correlation of 0.81), which correlates negatively with n_b (- 0.45) (Fig. 2). $CaCl_2$ addition
534 had no significant impact on the size of the dense regions (Fig. 7), while NaCl caused their
535 decrease, as shown by the correlation between $r_{b,}$ and the concentration of NaCl and therefore
536 diffusible Na and Cl (- 0.50, - 0.53 and - 0.45, respectively) (Fig. 2). The decrease of population
537 C also led to a decrease in size of the dense regions (correlation coefficient of 0.47 between
538 n_{cCaP} and r_b) (Fig. 2). Finally, it is interesting to note that n_b and r_b were inversely correlated (-
539 0.59) (Fig. 2), meaning that the more dense the regions within the micelle, the smaller the size of
540 these regions.

541 **3.1.2.3 Population C: CaP nanoclusters or protein inhomogeneities**

542 The mean radius of population C (r_c) ranged from 1.5 to 1.7 nm, for the set of suspensions
543 studied with a RSD of 3.1 % (Table 2). This indicates that this population is of similar size in
544 each suspension, regardless of the physico-chemical modifications applied. However, the
545 number per casein micelle, n_{cCaP}, varied from 75 to 244. Considering this population as CaP, the
546 number is close, although lower than the values of CaP nanoclusters in a native casein micelle
547 which has been calculated as ~285 by de Kruif, Huppertz, Urban & Petukhov, (2012). In our
548 experiments, the suspension of NPC powder in water caused ~20 % of the colloidal CaP to
549 dissolve (calculated based on the colloidal and diffusible contents of the CTRL sample) (Table
550 1). This reduction in CaP could explain the discrepancy with the data of de Kruif and colleagues.
551 The number observed, however, is consistent with the findings of Bouchoux et al., (2010), who
552 reported ~210 CaP nanoclusters per casein micelle.

If the population C scatterers were considered as protein inhomogeneities, their number per casein micelle varied from 140 to 453, which is about 17 times lower than the value found by Ingham et al., (2016) (Table 2). This difference may be due to the application of a simple sphere form factor in this study compared to the combination of a Sorensen form factor and hard sphere structure factor used by Ingham et al., (2016). Our approach was nevertheless sufficient to fit the SAXS pattern in the high q-region (Fig. 5). The properties of the C-scatterers *i.e.* constant size and varying number of C-scatterers per casein micelle indicated the disappearance of this population adhered to an "all-or-nothing" rule, where population C either "dissolved" completely upon modification of the environment or remained intact within the casein micelle.

According to the PCA analysis, n_{cCaP} correlated highly with pH (0.80), concentrations of colloidal Ca and Pi (0.86 and 0.80, respectively) and with concentration of diffusible Pi (- 0.84) (Fig. 2), indicating that the high q feature disappeared with the pH-induced dissolution of colloidal CaP. Similar pH induced changes in SAXS patterns of casein micelles were reported by Ingham et al., (2016) and Marchin et al., (2007). The disappearance of the high q feature was also observed when colloidal CaP was removed from the casein micelle by the use of chelating agents (EDTA or Na_3Cit) (Day et al., 2017; Ingham et al., 2016; Marchin et al., 2007; Pitkowski, Nicolai, & Durand, 2007). These correlations are therefore consistent with the assignment of this population as CaP nanoclusters, as suggested by Holt, de Kruif, Tuinier, & Timmins, (2003). The correlations between n_{cCaP} noted above are not inconsistent, however, with the hypothesis of Ingham et al. (2016) *i.e.* that this population of particles corresponds to protein inhomogeneities. In this case, protein inhomogeneities would be closely linked to micellar CaP. Dissolution of the CaP from the casein micelle would also induce the disruption of the protein inhomogeneities. Such an arrangement would be in agreement with the dual binding model of Horne, (1998), that considers CaP nanoclusters not only as crosslinking agents but also as charge neutralizers between casein chains that allow proteins to form more hydrophobic interactions. Further analysis in the form of cross comparisons between the evolution of the high

579 q SAXS shoulder and the specific intensity variation at q = 0.035 $Å^{-1}$ observed either in SANS or
580 resonant X-ray scattering would bring interesting information about this CaP nanocluster /
581 protein inhomogeneity dependency. Finally, n_{cCaP} correlated negatively with n_b (- 0.45) and with
582 $\Gamma_{s/l}$ (-0.43), and correlated positively with r_b (0.47) (Fig. 2). Whilst these correlations could arise
583 from a number of structural changes within the micelle, they suggest that protein from the
584 micelle is being released into the diffusible phase.

585 **3.2 Coagulation properties of the modified casein micelles**

586 The RCT and the maximum firmness of the gel, defined here as firmness, were determined for
587 the 27 suspensions using data obtained from the firmness curves (Fig. 8). These two
588 parameters were linked to the other colloidal and structural variables through PCA and multiple
589 linear regression analyses.

590 **3.2.1 Rennet clotting time**

591 The use of rennet made the 27 suspensions clot between 1.1 to 42.4 min (RSD of 113.5%)
592 (Table 3). This large variability was first ascribed to the variation in pH, as there was a significant
593 correlation between RCT and pH with a coefficient of 0.69 (Fig. 2). A consequence of the pH
594 decrease was the solubilization of the micellar Ca and Pi (section 3.1.1). Therefore RCT also
595 positively correlated with the concentration of colloidal Ca and Pi, and with diffusible Pi with
596 coefficients of 0.49, 0.61 and - 0.61, respectively (Fig. 2). A reduction in RCT as a result of a
597 decrease in pH has been well described in the literature (Choi et al., 2007; Daviau et al., 2000;
598 Karlsson et al., 2007; Zoon et al., 1989). This has been ascribed to the enhancement of enzyme
599 activity and a decrease in the electrostatic repulsion between paracaseinates at low pH that
600 favored aggregation.
601 A weaker but significant and positive correlation was also observed between diffusible Na and
602 RCT (0.39) (Fig. 2), meaning that an increased concentration of this ion in the diffusible phase
603 led to an increase in the RCT. Similar effects of added NaCl have been also reported by (Bulca
604 et al., 2016; Famelart et al., 1999; Grufferty & Fox, 1985; Karlsson et al., 2007; Sbodio et al.,

605 2006; Zhao & Corredig, 2015; Zoon et al., 1989) and were attributed to a decrease in the rate of
606 the rennet enzyme due to the screening of charges on κ-casein and the enzyme.
607
608 The negative correlations of RCT with τ and r_a (- 0.47 and – 0.53, respectively) (Fig. 2) indicated
609 that large micelles clotted more quickly than small ones, a finding that was opposite to those
610 made in the studies of Ekstrand, (1980) and Ford & Grandison, (1986). The increase of the
611 micellar size in the present study was a consequence of the pH decrease that caused the
612 micelles to swell and also potentially caused other structural changes. The correlation between
613 these two factors is probably a disguised effect of the pH and the effect of pH on both micelle
614 size and structure. In the two previous studies with opposing findings, the micelles were
615 fractionated according to their size by ultracentrifugation and did not undergo any physico-
616 chemical treatment, which could further explain these differences.
617 **3.2.2 Firmness of the rennet gel formed within the first 60 min of coagulation**
618 Although the firmness was highly variable, with an RSD of 34 % (Table 3) within the set of
619 suspensions, this variable did not correlate directly with the other colloidal and structural
620 characteristics of the casein micelle suspensions. Indeed, the firmness, concentrations of $CaCl_2$
621 and concentrations of diffusible Ca were the only well-projected variables as defined by the 3rd
622 and 4th dimensions of the PCA analysis (Fig. 4). Vectors representing concentrations of $CaCl_2$
623 and diffusible Ca were orthogonal to the vector for firmness, reflecting no correlations between
624 these variables. However, PCA estimates the first order correlations between variables, and
625 does not take into account the interactions that might exist between the different features.
626 A second statistical approach, multiple linear regression, was therefore used to assess the effect
627 of possible interactions between variables on the firmness of the rennet gels. Structural SAXS
628 features revealed to be excellent candidates for this complementary analysis for two reasons.
629 Firstly, these variables were unique and interesting descriptors reporting information at three
630 different structural levels: 1) the casein micelle, 40 to 60 nm in radius and previously described

631 as population A; 2) the dense regions, 6 to 22 nm in radius and previously described as
632 population B; 3) the CaP nanoclusters (or protein inhomogeneities), 1.5 to 1.7 nm in radius and
633 previously described as population C. Secondly, these variables correlated significantly with the
634 whole set of colloidal and mineral features determined by other techniques and constituted a
635 way to summarize the whole set of data. Therefore, r_a, n_b and n_{cCaP} were subject to linear
636 regression in order to define a predictive model of the firmness that considered the quadratic
637 effects and the second order interactions between these variables. For consistency, the values
638 of n_{cCaP} used in this statistical analysis were determined considering population C as CaP
639 nanoclusters. This would make no difference in the properties of the model, as there was a
640 proportional relationship linking n_{cCaP} for CaP nanoclusters and n_{cPI} for protein inhomogeneities.
641 Based on the experimental design, the following model equation was established to predict the
642 maximum firmness of the rennet gels made from the suspensions:
643 $$Firmness = 187.3 - 3.5 \times ra - 1.2 \times n_b - 0.9 \times n_{cCaP} + 0.02 \times (r_a \times n_c) \quad (9)$$
644 where r_a was the radius of the casein micelle, n_b and n_{cCaP} were the number of dense regions
645 and CaP nanoclusters per casein micelle, respectively. This model explained 68.5% of the
646 variability of the firmness. Statistical analysis also revealed that the interaction between r_a and n_c
647 (r_a x n_c) and the first order effect of n_b in this model were significant. These two contributions had
648 a statistical weight of 35.3% and 27 % in the model, respectively.
649 Figure 9.A and B. displays each suspension in the first four dimensions of the PCA. The
650 suspensions are colored according to their firmness (orange for weak, red for medium, black for
651 strong). Figure 9.A represents the evolution of firmness within the set of samples, defined by
652 PCs 3 and 4 with the arrow pointing in the direction of increasing firmness (the same direction as
653 seen in Figure 4). The negative coefficient assigned to n_b in the firmness equation model
654 indicates that the release of protein from the casein micelles led to the formation of weaker gels.
655 This direct effect is well illustrated when reading Figure 9.A from the bottom right corner

656 (suspension G, U - poor in dense regions and stronger gels) to the upper left corner (suspension
657 B - rich in dense regions and a weaker gel).
658 As described earlier, the release of dense regions was favored by the addition of NaCl and
659 limited by the addition of $CaCl_2$. The influence of NaCl on the firmness has been examined by
660 several groups but conflicting results have been reported. Consistent with the results reported
661 here, Famelart et al., (1999) and Grufferty & Fox (1985) did not observe any modification of the
662 moduli or the curd tension of the rennet gels upon addition of NaCl. However, Bulca et al.,
663 (2016) and Zhao & Corredig, (2015) reported a decrease in the firmness or stiffness of the
664 rennet gels. While Zoon et al., (1989) observed higher moduli for 8h aged gels supplemented in
665 NaCl but lower moduli was observed only 1 h after the addition of rennet to the milk,
666 corresponding to the experimental conditions of the present study. The negative effect of NaCl
667 on the firmness of rennet gels is poorly explained in the literature. A competition between Na^+
668 and Ca^{2+} has been proposed, as well as the screening of casein charges and in some cases, the
669 solubilization of the micellar CaP (Grufferty & Fox, 1985; Zhao & Corredig, 2015). Based on the
670 significant correlations that link n_b and NaCl and the significant negative effect of n_b on the
671 firmness of the rennet gel, we would argue that the decrease in firmness observed with the
672 addition of NaCl is due to the release of protein from the casein micelles. This explanation is
673 similar to that of Gaygadzhiev, Massel, Alexander, & Corredig, (2012), who found that the
674 addition of sodium caseinate to milk inhibited the aggregation of casein micelles. In this case,
675 the soluble dense regions may adsorb on the surface of the paracaseinate formed after rennet
676 addition, causing an increase in the steric repulsion between the rennet-altered particles which
677 would limit the aggregation phenomenon and the formation of a firm network.
678 In contrast, there is a general consensus that $CaCl_2$ addition increases gel firmness (Deeth &
679 Lewis, 2015; Sandra et al., 2012; Zoon et al., 1988). In this case, this improvement was
680 attributed to the ability of Ca to preserve the number of CaP bonds between the caseins within
681 the micelle but also within the casein gel network. It was demonstrated in section 3.1.2.2, that

682 $CaCl_2$ addition limited the release of dense regions, which consequently had a positive impact
683 on the firmness of the gels through the decrease of n_b.
684
685 The effect of the interaction between r_a and n_{cCaP} appears to be more subtle. The direct effect of
686 r_a could be seen in figure 9.B from the upper right corner (suspension M - small casein micelle)
687 to the bottom left corner (suspension A, D, O - large and swollen casein micelle). There were no
688 direct and simple consequences of r_a on the gel firmness. This can be illustrated by the medium
689 size micelles (center of the graph, suspensions B, S, V, L for instance) that can either form
690 weak, medium or strong gels. This result was quite consistent with the observation of Dalgleish,
691 Brinkhuis, & Payens, (1981) who found no dependence between the size of micelles and their
692 coagulation. Yet, several authors have reported that small casein micelles form stronger gels
693 (Ford & Grandison, 1986; Logan et al., 2015; Niki, Kohyama, Sano, & Nishinari, 1994). However,
694 in these studies, the micelles were in their native state because they were either isolated from
695 milk by ultracentrifugation or were in milk samples that were selected from cows who produced
696 small casein micelles. In contrast, the present study involved modifications to the environment
697 that affected the size of the casein micelles.
698 The direct effect of n_{cCaP} can be observed in figure 9.B from the upper left corner (suspension B
699 – poor in population C) to the bottom right corner (suspensions L, Y – rich in population C) but
700 no direct dependency of gel firmness on n_{cCaP} was observed. This population may be either CaP
701 nanoclusters or protein inhomogeneities. In both cases, the presence of such interactions,
702 whether they are mineral-protein or protein-protein interactions, would create more crosslinking
703 points resulting in a stronger gel network.
704 The literature reports a quadratic relationships between pH and rennet gel firmness, *i.e.* there is
705 a parabolic increase in the gel firmness with pH up to a maximum value, followed by a parabolic
706 decrease in firmness (Choi et al., 2007; Karlsson et al., 2007; Lucey, Johnson, & Horne, 2003;
707 Zoon et al., 1989). A change in pH modifies the ionization of individual amino acids, either

708 increasing or decreasing the electrostatic interactions between casein chains. A simultaneous
709 consequence is the solubilization of the micellar CaP at lower pH, which decreases the attractive
710 interactions between casein molecules. The addition of a chelating agent to milk or casein
711 suspension similarly leads to the solubilization of micellar CaP (de Kort et al., 2011; McCarthy et
712 al., 2017; Mizuno & Lucey, 2005; Pitkowski et al., 2007) and causes a decrease in the firmness
713 of the rennet gels (Choi et al., 2007).
714 At this point, it is important to remember that the variations of r_a and n_{cCaP} were not impacted by
715 only one factor (size fractionation, or pH, or chelating agent addition) but by the simultaneous
716 effect of three factors (pH, NaCl and $CaCl_2$). Therefore, the firmness modeling reveals that the
717 interaction between those variables should be considered. The interaction between r_a and n_{cCaP}
718 on the rennet gel firmness means that the firmness at a given r_a depended on n_{cCaP} and vice
719 versa. As an example to illustrate this interaction, suspensions containing medium sized casein
720 micelles (from 45 to 47 nm in radius) can lead to the formation of weaker gels if the amount of C-
721 particles is too low (suspension B). Yet these micelles formed medium strength gels
722 (suspensions P, E, C) if their C-particle content increased, or even stronger gels when those
723 casein micelles are rich in C-particles (suspensions X, I, T). Similarly, small casein micelles that
724 were rich in C-particles formed weaker gels (suspension W, K, M) but an increase in micelle size
725 led to an increase in gel firmness (suspension H, V, T). Large casein micelles, depleted in C
726 particles (suspension A, O, D) also formed weaker gels.
727

728 ## *4* Conclusion

729 The multifactorial experimental design applied here allowed the effect of three variables: pH,
730 NaCl and $CaCl_2$ on the colloidal and rennet coagulation properties of casein micelles to be
731 assessed and ranked. Variations in pH had the strongest influence on the mineral balance of the
732 casein micelles. A decrease in pH caused the colloidal CaP to solubilize. In contrast, NaCl
733 addition had no impact on the mineral content of the casein micelle. The solubilization of

734 colloidal CaP caused the micelle to shrink while the addition of NaCl reduced the size of the
735 casein micelle due to the release of small particles into the diffusible phase. The presence of
736 such particles, around 25 nm in diameter, was strongly supported by experimental SAXS data
737 combined with observations by cryo-TEM. These particles are believed to be part of the dense
738 regions described by Bouchoux et al. (2010); here they were observed both inside and outside
739 of the casein micelle. $CaCl_2$ had no effect on the casein micelle size but prevented disruption of
740 the dense regions within the micelle. The SAXS data also revealed the presence of a high-q
741 structural feature (the C-population), that were of a constant size (~1.6 nm in radius) but varied
742 in number with different environmental conditions. Their presence was strongly dependent to the
743 CaP content of the casein micelle. This feature could be assigned to the presence of either CaP
744 nanoclusters or protein inhomogeneities.
745 The renneting properties were most impacted by a decrease in pH, causing a reduction in RCT,
746 while NaCl supplementation led to longer RCT. Variations in gel firmness were more complex
747 but could be explained by considering the interactions between the size of the casein micelle,
748 the C-population and the dissociation of dense regions within the casein micelle.
749 Together the data presented here illustrate the complex interactions of three variables on the
750 properties of casein micelles in a simple model system relevant to products such as purified
751 casein micelles, fractionated from milk and prepared by diafiltration. This study provides a
752 framework that links existing literature on the effect of single variables and improves our
753 understanding of how the properties of casein micelles can be manipulated to control micelle
754 size, structure and functional properties. It also provides a basis for future studies to examine
755 casein micelles in more complex dairy product matrices and as a function of processing.
756

757 **5 Acknowledgment**

758 Acknowledgements are given to François Boué for the interesting discussions regarding the
759 modeling of the SAXS data, to Arlette Leduc for assistance in the analysis of the minerals, to Mi

760 Xu for assistance with data collection at the Australian Synchrotron and the Biological Optical
761 Microscopy Platform (BOMP) at the Bio21 Molecular Science and Biotechnology Institute for
762 access to equipment.
763 Fundings: This work was supported by the French Dairy Interbranch Organization (CNIEL) for
764 their financial support and by Chr Hansen through the loan of a Chymograph®. Sally Gras and
765 Lydia Ong are supported by the Australian Research Council's Industrial Transformation
766 Research Program (ITRP) funding scheme (project number IH120100005). The ARC Dairy
767 Innovation Hub is a collaboration between the University of Melbourne, The University of
768 Queensland and Dairy Innovation Australia Ltd. The SAXS experiments were undertaken on the
769 SAXS/WAXS beamline at the Australian Synchrotron, Victoria, Australia (Proposal No.
770 AS163/SAXS/11019).
771

772 **6 References**

773 Abdi, H., & Williams, L. J. (2010). Principal component analysis. *Wiley Interdisciplinary Reviews:*
774 *Computational Statistics*, *2*(4), 433–459.
775 Aoki, T., Umeda, T., & Nakao, T. (1999). Effect of sodium chloride on the properties of casein
776 micelles, *Milchwissenschaft*, 54(*2)*, 91–93.
777 Bouchoux, A., Gésan-Guiziou, G., Pérez, J., & Cabane, B. (2010). How to squeeze a sponge:
778 casein micelles under osmotic stress, a SAXS study. *Biophysical Journal*, *99*(11), 3754–3762.
779 Bouchoux, A., Ventureira, J., Gésan-Guiziou, G., Garnier-Lambrouin, F., Qu, P., Pasquier, C.,
780 Pézennec, S., Schweins, R., Cabane, B. (2015). Structural heterogeneity of milk casein micelles:
781 a SANS contrast variation study. *Soft Matter*, *11*(2), 389–399.
782 Broyard, C., & Gaucheron, F. (2015). Modifications of structures and functions of caseins: a
783 scientific and technological challenge. *Dairy Science & Technology*, 95(6), 831-862

784 Bulca, S., Wolfschoon-Pombo, A., & Kulozik, U. (2016). Rennet coagulation properties of UHT-
785 treated phosphocasein dispersions as a function of casein and NaCl concentrations.
786 *International Journal of Dairy Technology*, *69*(3), 328–336.
787 Chen, Y.-Y., Peng, B., Yang, Q., Glew, M. D., Veith, P. D., Cross, K. J., Goldie, K.N., Chen, D.,
788 O'Brien-Simpsion, N., Dashper, S.G., Reynolds, E. C. (2011). The outer membrane protein LptO
789 is essential for the O-deacylation of LPS and the co-ordinated secretion and attachment of A-
790 LPS and CTD proteins in Porphyromonas gingivalis: LptO-dependent maturation of A-LPS and
791 CTD proteins. *Molecular Microbiology*, *79*(5), 1380–1401.
792 Choi, J., Horne, D. S., & Lucey, J. A. (2007). Effect of insoluble calcium concentration on rennet
793 coagulation properties of milk. *Journal of Dairy Science*, *90*(6), 2612–2623.
794 Dalgleish, D. G., Brinkhuis, J., & Payens, T. A. J. (1981). The coagulation of differently sized
795 casein micelles by rennet. *European Journal of Biochemistry*, *119*(2), 257–261.
796 Dalgleish, D. G., & Corredig, M. (2012). The Structure of the Casein Micelle of Milk and Its
797 Changes During Processing. *Annual Review of Food Science and Technology*, *3*(1), 449–467.
798 Dalgleish, D. G., & Law, A. J. R. (1989). pH-Induced dissociation of bovine casein micelles. II.
799 Mineral solubilization and its relation to casein release. *Journal of Dairy Research*, *56*(05), 727.
800 Daviau, C., Famelart, M.-H., Pierre, A., Goudedranche, H., & Maubois, J.-L. (2000). Rennet
801 coagulation of skim milk and curd drainage: effect of pH, casein concentration, ionic strength
802 and heat treatment. *Le Lait*, *80*(4), 397–415.
803 Day, L., Raynes, J. K., Leis, A., Liu, L. H., & Williams, R. P. W. (2017). Probing the internal and
804 external micelle structures of differently sized casein micelles from individual cows milk by
805 dynamic light and small-angle X-ray scattering. *Food Hydrocolloids*, *69*, 150–163.
806 de Kort, E., Minor, M., Snoeren, T., van Hooijdonk, T., & van der Linden, E. (2011). Effect of
807 calcium chelators on physical changes in casein micelles in concentrated micellar casein
808 solutions. *International Dairy Journal*, *21*(12), 907–913.
809 de Kruif, C. G. (1999). Casein micelle interactions. *International Dairy Journal*, *9*(3–6), 183–188.

de Kruif, C. G. (2014). The structure of casein micelles: a review of small-angle scattering data. *Journal of Applied Crystallography*, *47*(5), 1479–1489.

de Kruif, C. G., & Zhulina, E. B. (1996). k-casein as a polyelectrolyte brush on the surface of casein micelles. *Colloids and Surfaces A: Physicochemical and Engineering Aspects*, *117*(1–2), 151–159.

Deeth, H. C., & Lewis, M. J. (2015). Practical consequences of calcium addition to and removal from milk and milk products. *International Journal of Dairy Technology*, *68*(1), 1–10.

Ekstrand, B., Larsson-Raznikiewicz, M., Perlmann, C. (1980). Casein micelle size and composition related to the enzymatic coagulation process. *Biochimica et Biophysica Acta-General Subjects*, *630*(3), 361–366.

Famelart, M.-H., Le Graet, Y., & Raulot, K. (1999). Casein micelle dispersions into water, NaCl and CaCl2: physicochemical characteristics of micelles and rennet coagulation. *International Dairy Journal*, *9*, 293–297.

Famelart, M.-H., Lepesant, F., Gaucheron, F., Le Graet, Y., & Schuck, P. (1996). pH-Induced physicochemical modifications of native phosphocaseinate suspensions: Influence of aqueous phase. *Le Lait*, *76*(5), 445–460.

Ford, G. D., & Grandison, A. S. (1986). Effect of size of casein micelles on coagulation properties of skim milk. *Journal of Dairy Research*, *53*(01), 129.

Gaucheron, F. (2004). *Minéraux et produits laitiers*. Paris: Technique & Documentation.

Gaygadzhiev, Z., Massel, V., Alexander, M., & Corredig, M. (2012). Addition of sodium caseinate to skim milk inhibits rennet-induced aggregation of casein micelles. *Food Hydrocolloids*, *26*(2), 405–411.

Grufferty, M. B., & Fox, P. F. (1985). Effect of added NaCl on some physicochemical properties of milk, *Irish Journal of Food Science and Technology*, *9(1)*, 1–9.

834 Guinee, T. P., Gorry, C. B., O'Callaghan, D. J., O'Kennedy, B. T., O'Brie, N., Fenelon, M. A.
835 (1997). The effects of composition and some processing treatments on the rennet coagulation
836 properties of milk. *International Journal of Dairy Technology. 50(3)*, 99-106
837 Holt, C., Carver, J. A., Ecroyd, H., & Thorn, D. C. (2013). Invited review: Caseins and the casein
838 micelle: Their biological functions, structures, and behavior in foods. *Journal of Dairy Science*,
839 *96*(10), 6127–6146.
840 Holt, C, de Kruif, C. G., Tuinier, R., & Timmins, P. A. (2003). Substructure of bovine casein
841 micelles by small-angle X-ray and neutron scattering. *Colloids and Surfaces A: Physicochemical*
842 *and Engineering Aspects*, *213*(2–3), 275–284.
843 Holt, C., Timmins, P. A., Errington, N., & Leaver, J. (1998). A core-shell model of calcium
844 phosphate nanoclusters stabilized by beta-casein phosphopeptides, derived from sedimentation
845 equilibrium and small-angle X-ray and neutron-scattering measurements. *European Journal of*
846 *Biochemistry*, *252*(1), 73–78.
847 Holt, C. (2016). Casein and casein micelle structures, functions and diversity in 20 species.
848 *International Dairy Journal*, *60*, 2–13.
849 Holt, C., & Horne, D. S. (1996). The hairy casein micelle : Evolution of the concept and its
850 implications for dairy technology. *Nederlands Melk En Zuiveltijdschrift*, *50*(2), 85–111.
851 Horne, D. S. (1998). Casein interactions: casting light on the black boxes, the structure in dairy
852 products. *International Dairy Journal*, *8*(3), 171–177.
853 Horne, D. S. (2017). A balanced view of casein interactions. *Current Opinion in Colloid &*
854 *Interface Science*, *28*, 74–86.
855 Ingham, B., Erlangga, G. D., Smialowska, A., Kirby, N. M., Wang, C., Matia-Merino, L.,
856 Haverkamp, R.G., Carr, A. J. (2015). Solving the mystery of the internal structure of casein
857 micelles. *Soft Matter*, *11*(14), 2723–2725.
858 International Dairy Federation. (2014). Milk and milk products - Determination of nitrogen content
859 - Part 1: Kjeldahl principle and crude protein calculation.

860 Ingham, B., Smialowska, A., Erlangga, G. D., Matia-Merino, L., Kirby, N. M., Wang, C.,
861 Haverkamp, R. G., Carr, A. J. (2016). Revisiting the interpretation of casein micelle SAXS data.
862 *Soft Matter*, *12*(33), 6937–6953.
863 Jolliffe I. (2011) *Principal Component Analysis.* Berlin: Springer
864 Karlsson, A. O., Ipsen, R., & Ardö, Y. (2007). Influence of pH and NaCl on rheological properties
865 of rennet-induced casein gels made from UF concentrated skim milk. *International Dairy Journal*,
866 *17*(9), 1053–1062.
867 Karlsson, A. O., Ipsen, R., Schrader, K., & Ardö, Y. (2005). Relationship between physical
868 properties of casein micelles and rheology of skim milk concentrate. *Journal of Dairy Science*,
869 *88*(11), 3784–3797.
870 Lazzaro, F., Saint-Jalmes, A., Violleau, F., Lopez, C., Gaucher-Delmas, M., Madec, M.-N.,
871 Beaucher, E., Gaucheron, F. (2017). Gradual disaggregation of the casein micelle improves its
872 emulsifying capacity and decreases the stability of dairy emulsions. *Food Hydrocolloids*, *63*,
873 189–200.
874 Le Graet, Y., & Brulé, G. (1993). Les équilibres minéraux du lait : influence du pH et de la force
875 ionique, *Le Lait*, *73(1)*, 51–60.
876 Le Graet, Y., & Gaucheron, F. (1999). pH-induced solubilization of minerals from casein
877 micelles: influence of casein concentration and ionic strength, *Journal of Dairy Research*, *66(2)*,
878 215–224.
879 Le Ray, C., Maubois, J.-L., Gaucheron, F., Brulé, G., Pronnier, P., & Garnier, F. (1998). Heat
880 stability of reconstituted casein micelle dispersions: changes induced by salt addition. *Le Lait*,
881 *78*(4), 375–390.
882 Lê, S., Josse, J., & Husson, F. (2008). FactoMineR: An R package for multivariate analysis.
883 *Journal of Statistical Software*, *25*(1).

884 Logan, A., Leis, A., Day, L., Øiseth, S. K., Puvanenthiran, A., & Augustin, M. A. (2015). Rennet
885 gelation properties of milk: Influence of natural variation in milk fat globule size and casein
886 micelle size. *International Dairy Journal*, *46*, 71–77.
887 Lucey, J. A. (2002). Formation and physical properties of milk protein gels. *Journal of Dairy*
888 *Science*, *85*(2), 281–294.
889 Lucey, J. A., Johnson, M. E., & Horne, D. S. (2003). Invited review: Perspectives on the basis of
890 the rheology and texture properties of cheese. *Journal of Dairy Science*, *86*(9), 2725–2743.
891 Marchin, S., Putaux, J.-L., Pignon, F., & Léonil, J. (2007). Effects of the environmental factors on
892 the casein micelle structure studied by cryo transmission electron microscopy and small-angle x-
893 ray scattering/ultrasmall-angle x-ray scattering. *The Journal of Chemical Physics*, *126*(4),
894 045101.
895 McCarthy, N. A., Power, O., Wijayanti, H. B., Kelly, P. M., Mao, L., & Fenelon, M. A. (2017).
896 Effects of calcium chelating agents on the solubility of milk protein concentrate. *International*
897 *Journal of Dairy Technology*, *70*(3), 415–423.
898 Mishra, R. I., Govindasamy-Lucey, S. E., Lucey, J. A. (2005). Rheological properties of rennet-
899 induced gels during the coagualtion and cutting process: impact of processing conditions.
900 *Journal of texture studies. 36(2),* 190-212.
901 Mizuno, R., & Lucey, J. A. (2005). Effects of emulsifying salts on the turbidity and calcium-
902 phosphate–protein interactions in casein micelles. *Journal of Dairy Science*, *88*(9), 3070–3078.
903 Moitzi, C., Menzel, A., Schurtenberger, P., & Stradner, A. (2011). The pH induced Sol–Gel
904 transition in skim milk revisited. A detailed study using time-resolved light and X-ray scattering
905 experiments. *Langmuir*, *27*(6), 2195–2203.
906 Müller-Buschbaum, P., Gebhardt, R., Roth, S. V., Metwalli, E., & Doster, W. (2007). Effect of
907 calcium concentration on the structure of casein micelles in thin films. *Biophysical Journal*, *93*(3),
908 960–968.

Niki, R., Kohyama, K., Sano, Y., & Nishinari, K. (1994). Rheological study on the rennet-induced gelation of casein micelles with different sizes. *Polymer Gels and Networks*, *2*(2), 105–118.

Ouanezar, M., Guyomarc'h, F., & Bouchoux, A. (2012). AFM imaging of milk casein micelles: Evidence for structural rearrangement upon acidification. *Langmuir*, *28*(11), 4915–4919.

Philippe, M, Le Graet, Y., & Gaucheron, F. (2005). The effects of different cations on the physicochemical characteristics of casein micelles. *Food Chemistry*, *90*(4), 673–683.

Philippe, Marine, Gaucheron, F., Le Graet, Y., Michel, F., & Garem, A. (2003). Physicochemical characterization of calcium-supplemented skim milk. *Le Lait*, *83*(1), 45–59.

Pierre, A., Fauquant, J., Le Graet, Y., & Maubois, J.-L. (1992). Préparation de phosphocaséinate natif par microfiltration sur membrane. *Le Lait*, 72 (5), 461–474.

Pignon, F., Belina, G., Narayanan, T., Paubel, X., Magnin, A., & Gésan-Guiziou, G. (2004). Structure and rheological behavior of casein micelle suspensions during ultrafiltration process. *The Journal of Chemical Physics*, *121*(16), 8138-8146.

Pitkowski, A., Nicolai, T., & Durand, D. (2007). Scattering and turbidity study of the dissociation of the casein by calcium chelation. *Biomacromolecules*, *9*, 369–375.

Priyashantha, H., Lundh, Å., Höjer, A., Hetta, M., Johansson, M., and Langton, M. (2019). Interactive effects of casein micelle size and calcium and citrate content on rennet-induced coagulation in bovine milk. Journal of Texture Studies,1-12.

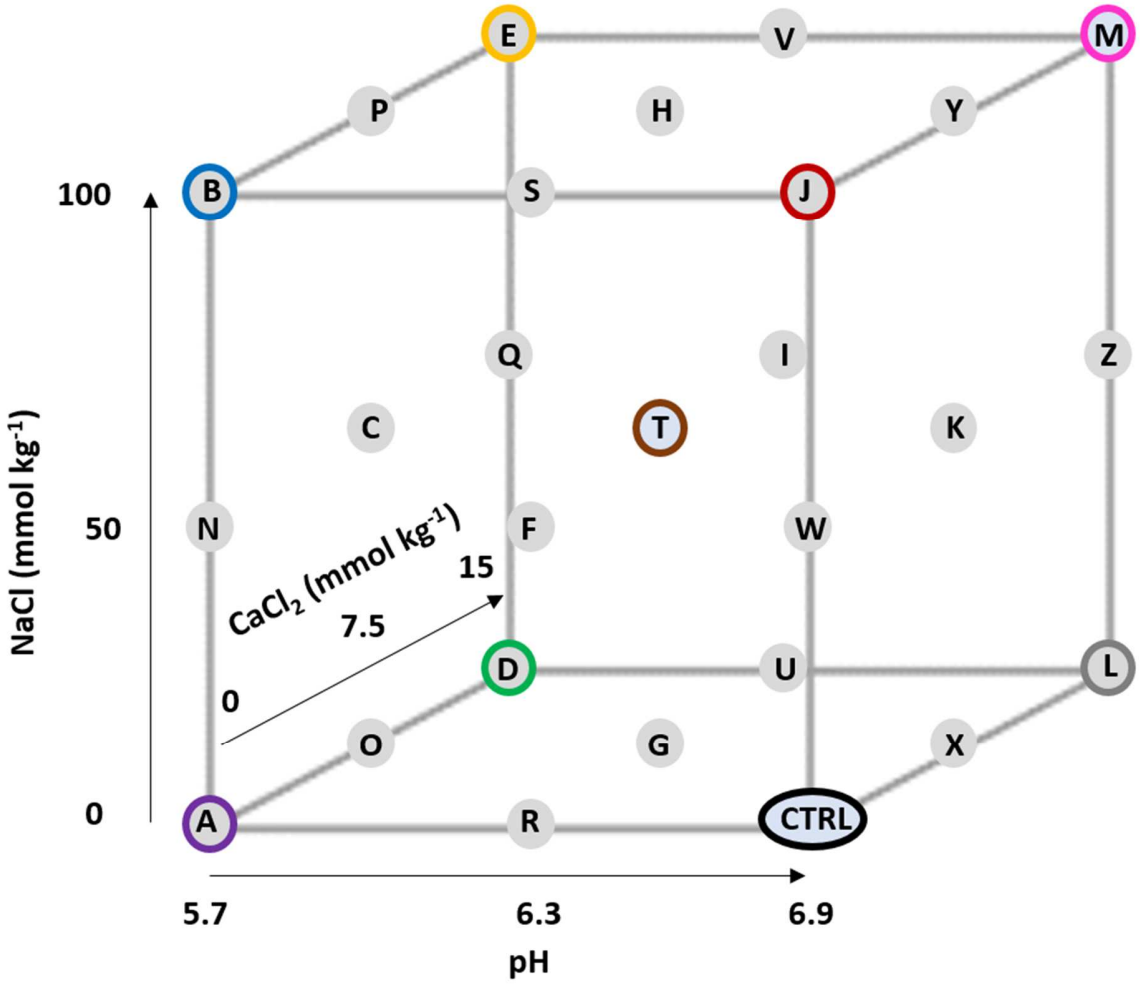
Sandra, S., Ho, M., Alexander, M., & Corredig, M. (2012). Effect of soluble calcium on the renneting properties of casein micelles as measured by rheology and diffusing wave spectroscopy. *Journal of Dairy Science*, *95*(1), 75–82.

Sbodio, O. A., Tercero, E. J., Coutaz, R., & Revelli, G. R. (2006). Effect of rennet and sodium chloride concentration on milk coagulation properties. *Ciencia Y Tecnologia Alimentaria*, *5*(3), 182–188.

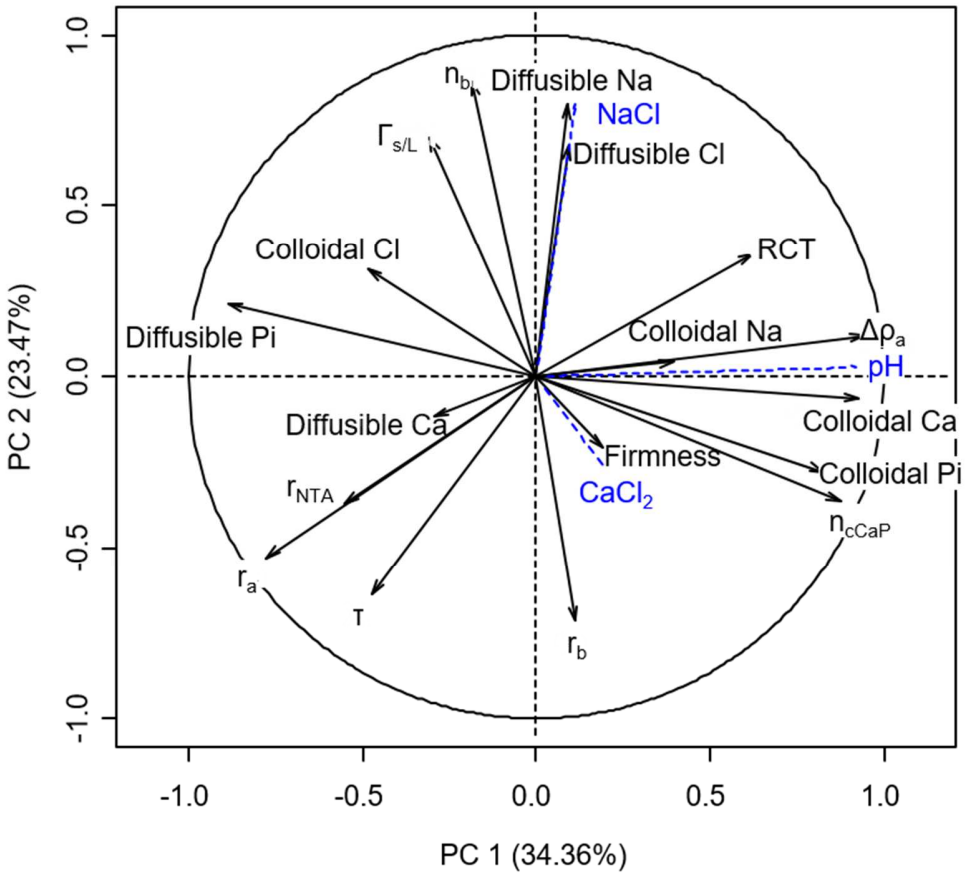
Schmidt, D. G. (1982). *Developments in Dairy Chemistry: 1. Proteins* (P. F. Fox). London: Applied Science Publishers.

935 Schuck, P., Piot, M., Méjean, S., Le Graet, Y., Fauquant, J., Brulé, G., & Maubois, J. L. (1994).
936 Déshydratation par atomisation de phosphocaséinate natif obtenu par microfiltration sur
937 membrane. *Le Lait*, *74*(5), 375–388.
938 Schuck, P., Dolivet, A., Jeantet, R., (2012). Analytical Methods for Food and Dairy Powders.
939 Oxford: John Wiley & Sons
940 Schulz, G. V. (1935). Highly polymerized compounds. CXXII. The relation between reaction rate
941 and composition of the reaction product in macropolymerization processes. *Zeitschrift für*
942 *Physikalische Chemie, B30*, 379–398.
943 Shukla, A., Narayanan, T., & Zanchi, D. (2009). Structure of casein micelles and their
944 complexation with tannins. *Soft Matter*, *5*(15), 2884.
945 Silva, N. N., Piot, M., de Carvalho, A. F., Violleau, F., Fameau, A.-L., & Gaucheron, F. (2013).
946 pH-induced demineralization of casein micelles modifies their physico-chemical and foaming
947 properties. *Food Hydrocolloids*, *32*(2), 322–330.
948 Thorn, D. C., Meehan, S., Sunde, M., Rekas, A., Gras, S. L., MacPhee, C. E., Dobson, C. M.,
949 Wilson, M. R., Carver, J. A. (2005). Amyloid fibril formation by bovine milk κ-Casein and Its
950 inhibition by the molecular haperones α_S - and β-Casein. *Biochemistry*, *44*(51), 17027–17036.
951 Tran Le, T., Saveyn, P., Hoa, H. D., & Van der Meeren, P. (2008). Determination of heat-
952 induced effects on the particle size distribution of casein micelles by dynamic light scattering and
953 nanoparticle tracking analysis. *International Dairy Journal*, *18*(12), 1090–1096.
954 Tuinier, R., & de Kruif, C. G. (2002). Stability of casein micelles in milk. *The Journal of Chemical*
955 *Physics*, *117*(3), 1290–1295.
956 Udabage, P., McKinnon, I. R., & Augustin, M. A. (2000). Mineral and casein equilibria in milk:
957 effects of added salts and calcium-chelating agents, *Journal of Dairy Research, 67(3)*, 361–370.
958 Udabage, P., McKinnon, I. R., Augustin, M. A. (2001). Effects of mineral salts and calcium
959 chelating agents on the gelation of renneted skim milk. *Journal of Dairy Science. 84(7),* 1569-75.

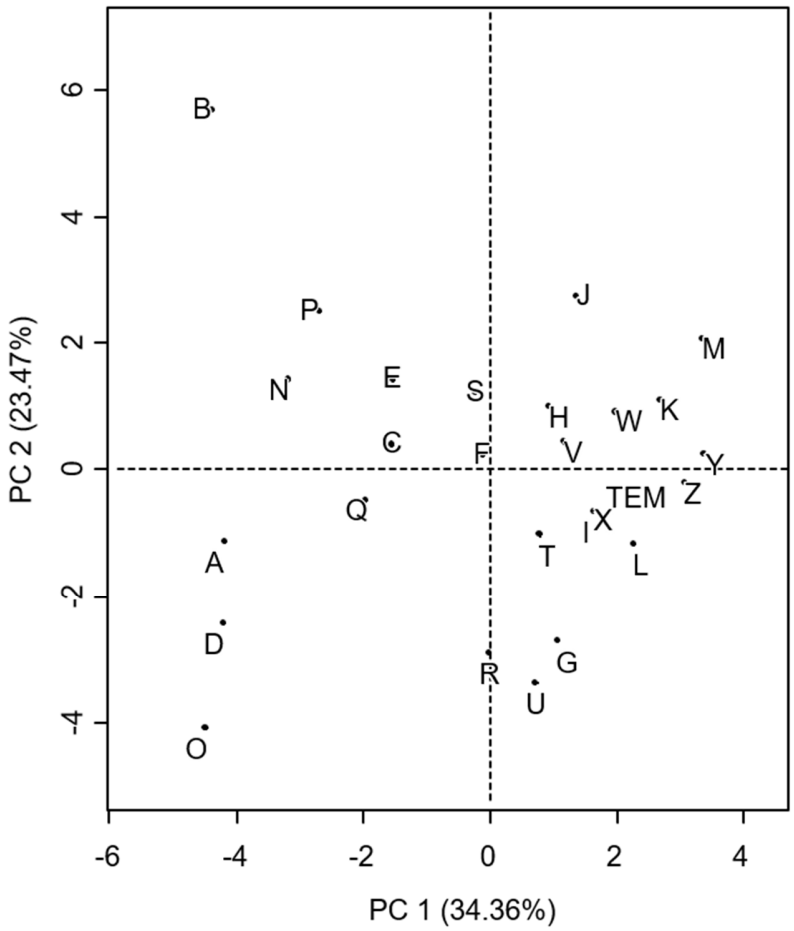
960 van Hooydonk, A. C. M., Boerrigter, I. J., & Hagedoorn, H. G. (1986). pH-induced physico-
961 chemical changes of casein micelles in milk and their effect on renneting. 2. Effect of pH on
962 renneting of milk, *Netherland Milk and Dairy Journal, 40*, 297–313.
963 Walstra, P. (1999). Casein sub-micelles: do they exist? *International Dairy Journal*, *9*(3–6), 189–
964 192.
965 Wold, S., Esbensen, K., & Geladi, P. (1987). Principal component analysis. *Chemometrics and*
966 *Intelligent Laboratory Systems*, *2*(1–3), 37–52.
967 Zhao, Z., & Corredig, M. (2015). Changes in the physico-chemical properties of casein micelles
968 in the presence of sodium chloride in untreated and concentrated milk protein. *Dairy Science &*
969 *Technology*, *95*(1), 87–99.
970 Zoon, P., van Vliet, T., & Walstra, P. (1988). Rheological properties of rennet-induced skim milk
971 gels. 3. The effect of calcium and phosphate, *Netherland Milk and Dairy Journal, 42*, 295–312.
972 Zoon, P., van Vliet, T., & Walstra, P. (1989). Rheological properties of rennet-induced skim milk
973 gels. 4. The effect of pH and NaCl, *Netherland Milk and Dairy Journal, 43*, 17–34.


E
V
M
P
H
Y
100
B
S
J
Q
I
Z
C
T
K
50
N
F
W
CaCl2 (mmol kg-1)
15
7.5
0
D
U
L
O
G
X
0
A
R
CTRL
5.7
6.3
6.9
pH
NaCl (mmol kg-1)

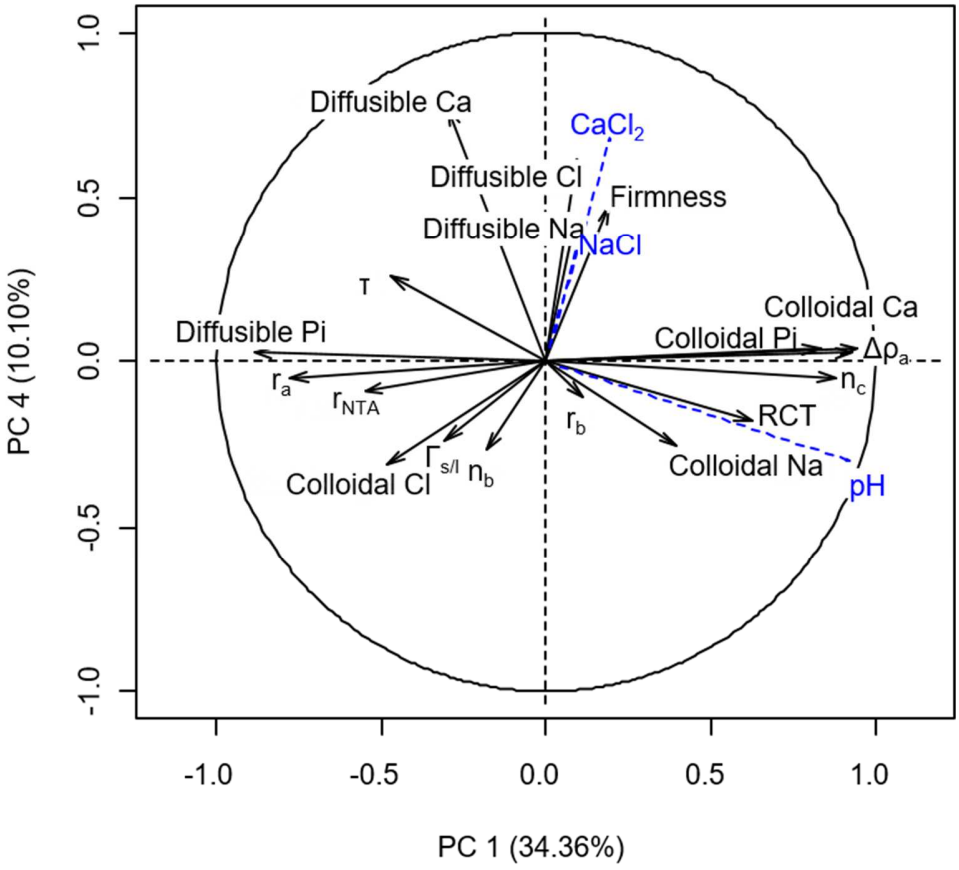
A.


PC 2 (23.47%)
PC 1 (34.36%)
1.0
0.5
0.0
-0.5
-1.0
n_{b_i}
Diffusible Na
NaCl
$\Gamma_{s/L}$
Diffusible Cl
Colloidal Cl
RCT
Diffusible Pi
Colloidal Na
$\Delta\rho_a$
pH
Diffusible Ca
Colloidal Ca
Firmness
Colloidal Pi
r_{NTA}
$CaCl_2$
n_{cCaP}
r_a
τ
r_b

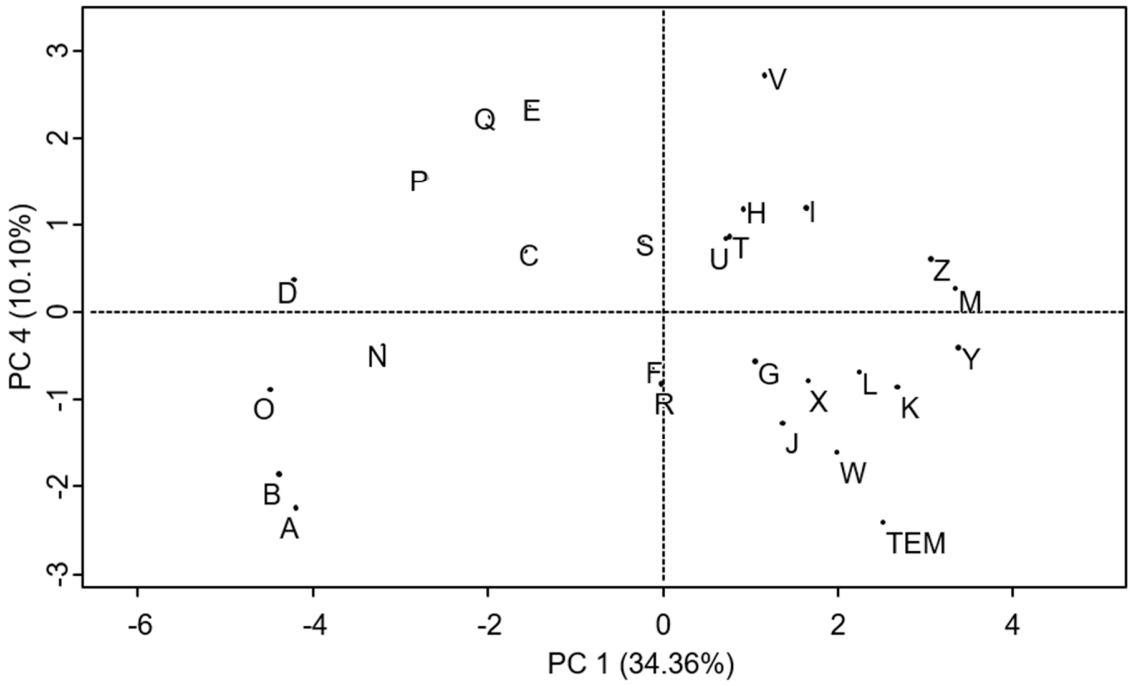
B.


B
P
J
M
N
E
S
H
W
K
C
F
V
Y
TEM
Z
Q
X
I
A
T
L
D
G
R
U
O
PC 2 (23.47%)
PC 1 (34.36%)
6
4
2
0
-2
-4
-6
-4
-2
0
2
4

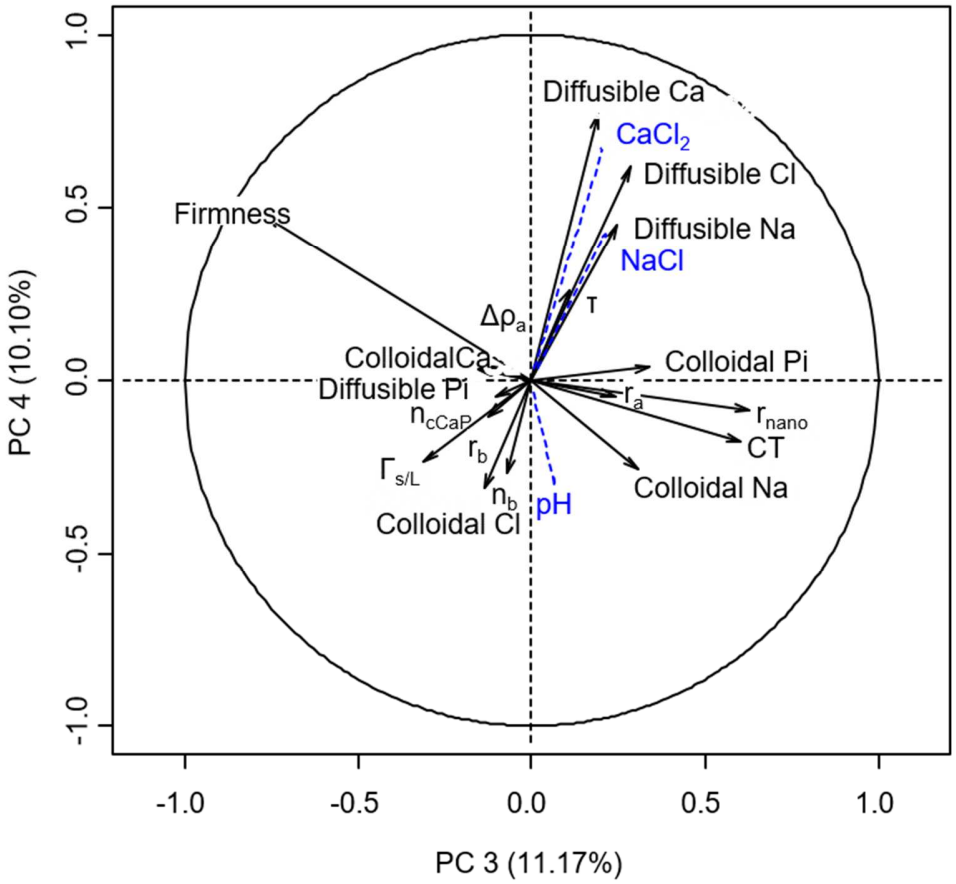
A.

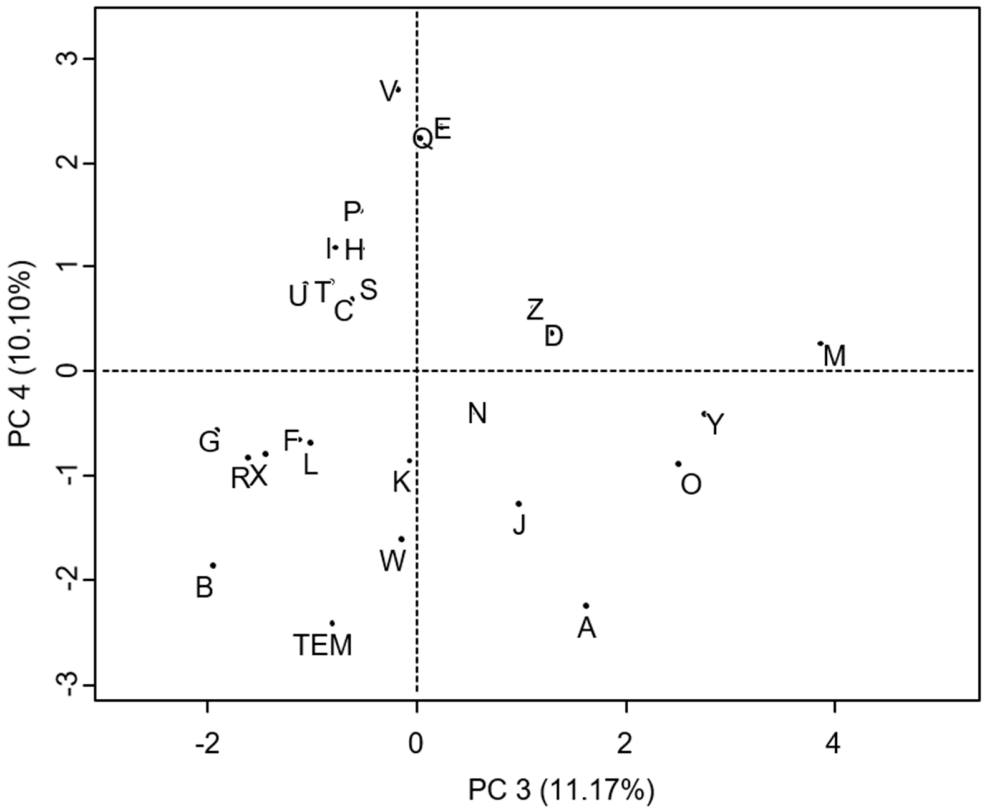

Diffusible Ca
CaCl2
Diffusible Cl
Firmness
Diffusible Na
NaCl
τ
Colloidal Ca
Diffusible Pi
Colloidal Pi
Δρa
nc
ra
rNTA
rb
RCT
Γs/l nb
Colloidal Cl
Colloidal Na
pH
PC 4 (10.10%)
PC 1 (34.36%)
1.0
0.5
0.0
-0.5
-1.0
-1.0
-0.5
0.0
0.5
1.0

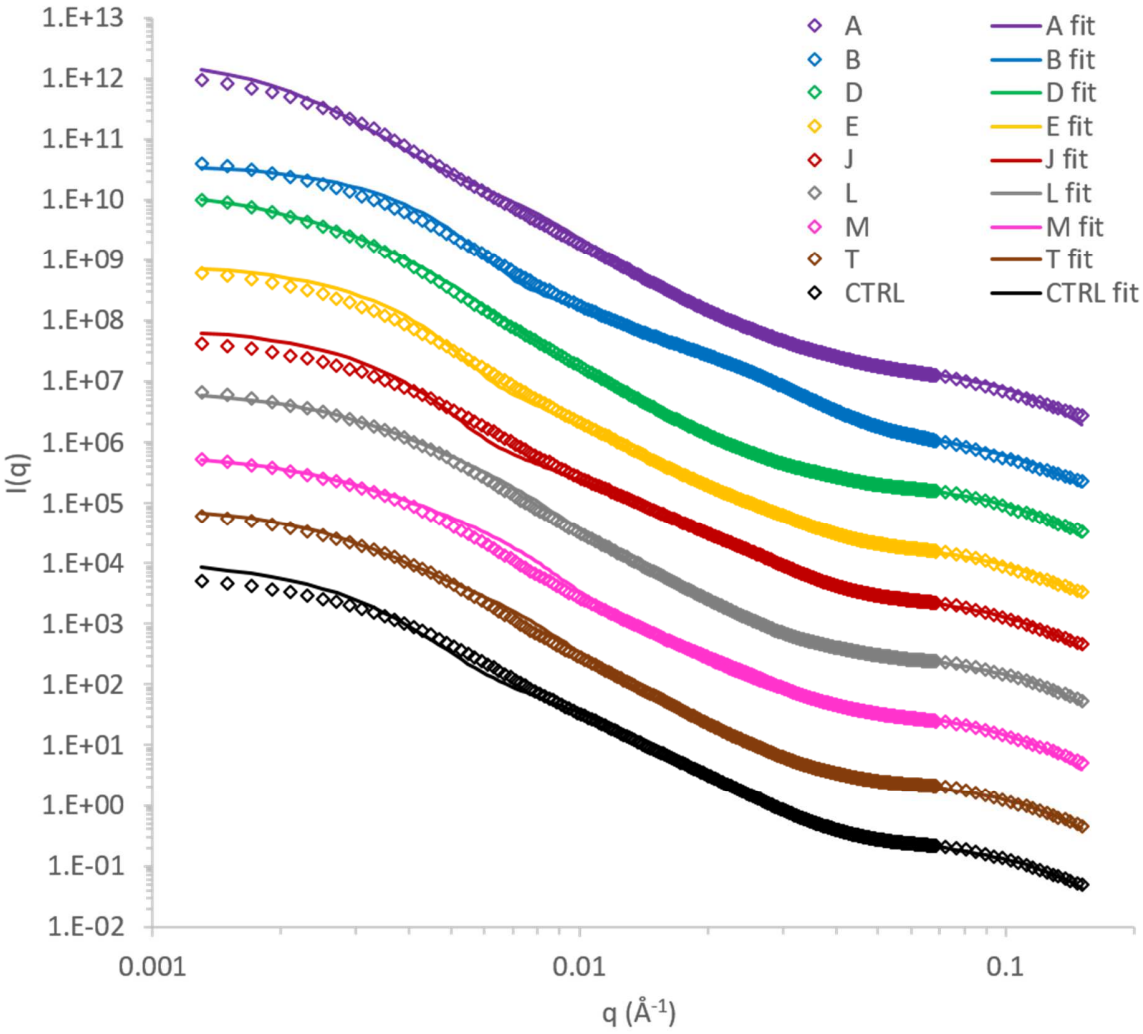
B.

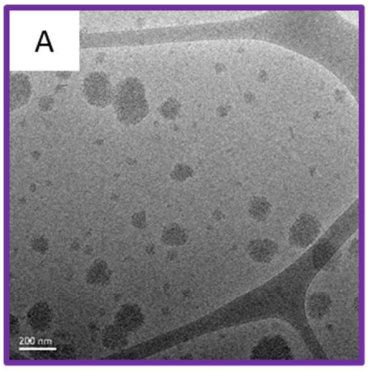

PC 4 (10.10%)
PC 1 (34.36%)
3
2
1
0
-1
-2
-3
-6
-4
-2
0
2
4
V
Q
E
P
H
I
C
S
U
T
Z
D
M
N
Y
F
G
L
O
R
X
K
J
W
B
A
TEM

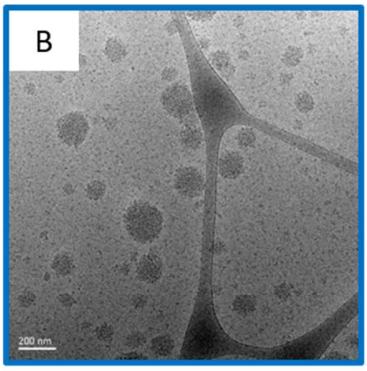
A.

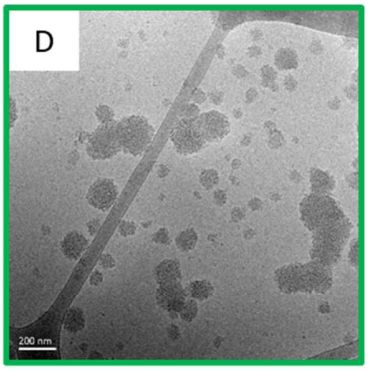

Diffusible Ca
CaCl2
Diffusible Cl
Diffusible Na
NaCl
Firmness
τ
Δpa
ColloidalCa
Diffusible Pi
Colloidal Pi
ra
rnano
CT
ncCaP
rb
Γs/L
nb
pH
Colloidal Na
Colloidal Cl
1.0
0.5
0.0
-0.5
-1.0
PC 4 (10.10%)
PC 3 (11.17%)

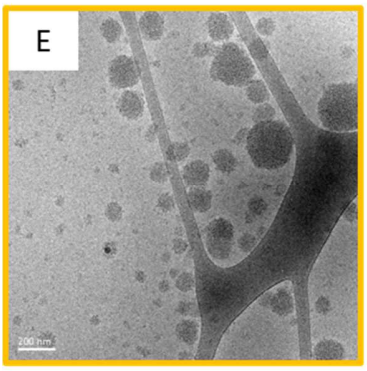

PC 4 (10.10%)
PC 3 (11.17%)
3
2
1
0
-1
-2
-3
-2
0
2
4
V
Q
E
P
I
H
U
T
C
S
Z
D
M
N
Y
G
F
L
R
X
K
O
J
W
B
A
TEM

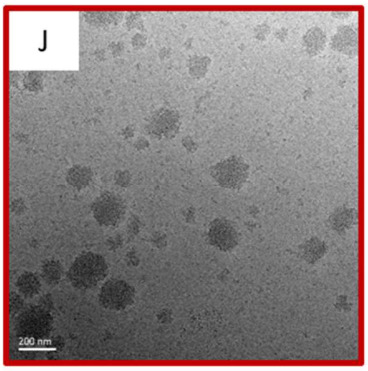

1.E+13
1.E+12
1.E+11
1.E+10
1.E+09
1.E+08
1.E+07
1.E+06
1.E+05
1.E+04
1.E+03
1.E+02
1.E+01
1.E+00
1.E-01
1.E-02
I(q)
0.001
0.01
0.1
q (Å-1)
A
B
D
E
J
L
M
T
CTRL
A fit
B fit
D fit
E fit
J fit
L fit
M fit
T fit
CTRL fit

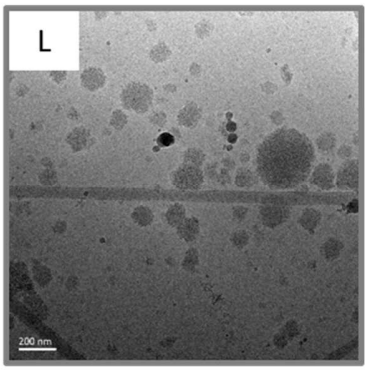

A
200 nm

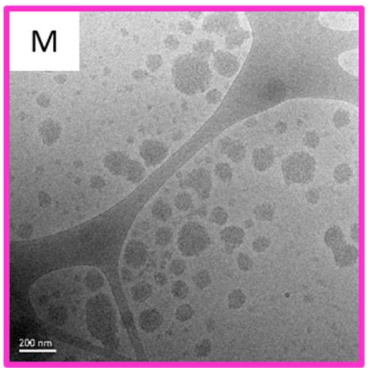

B
200 nm

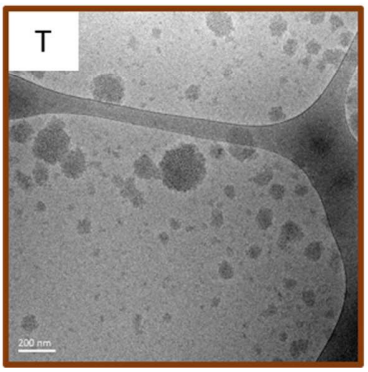

D
200 nm

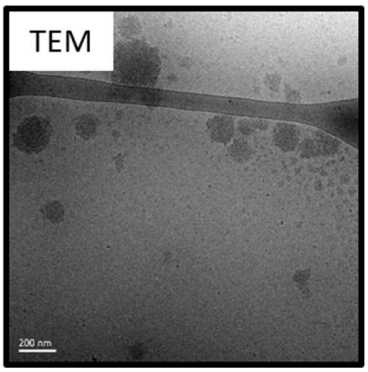

E
200 nm


J
200 nm

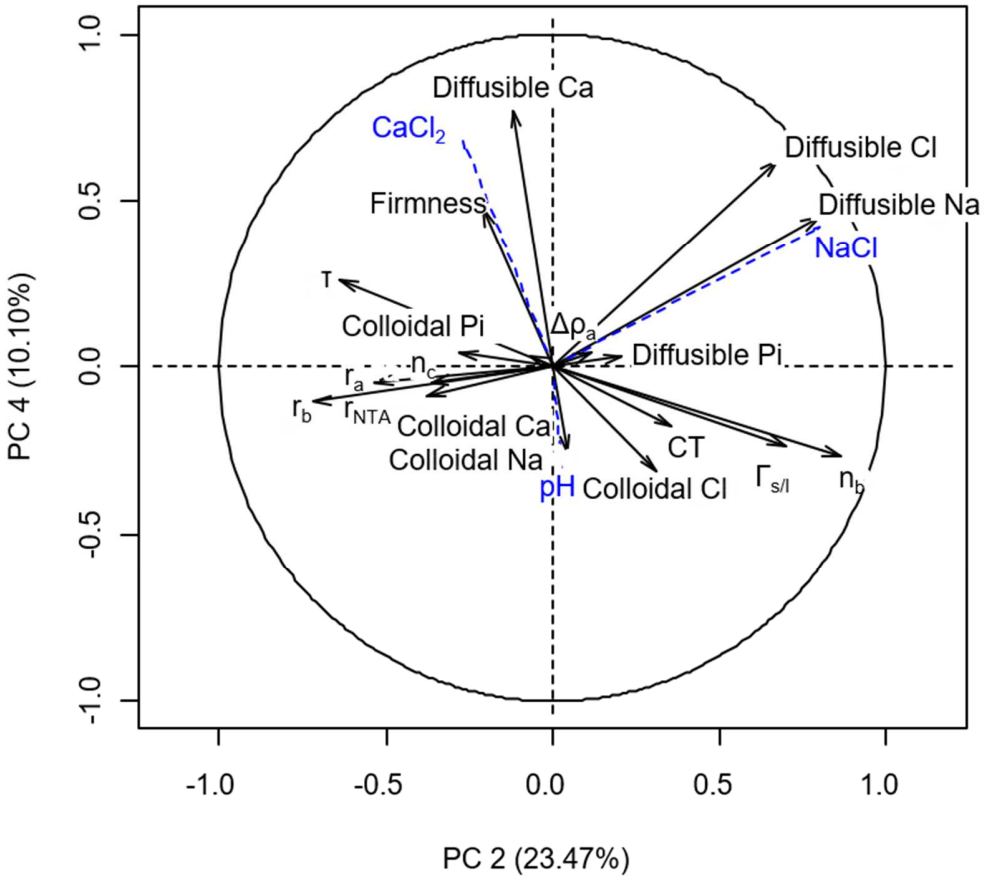

L
200 nm


M
200 nm

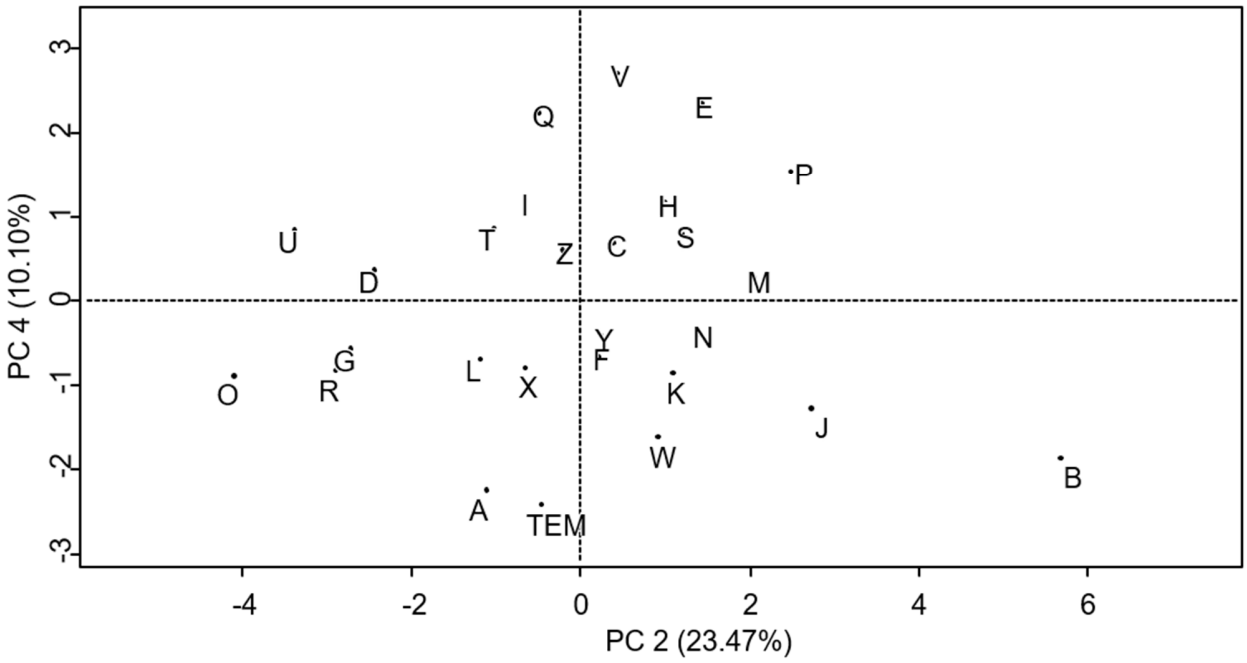

T
200 nm

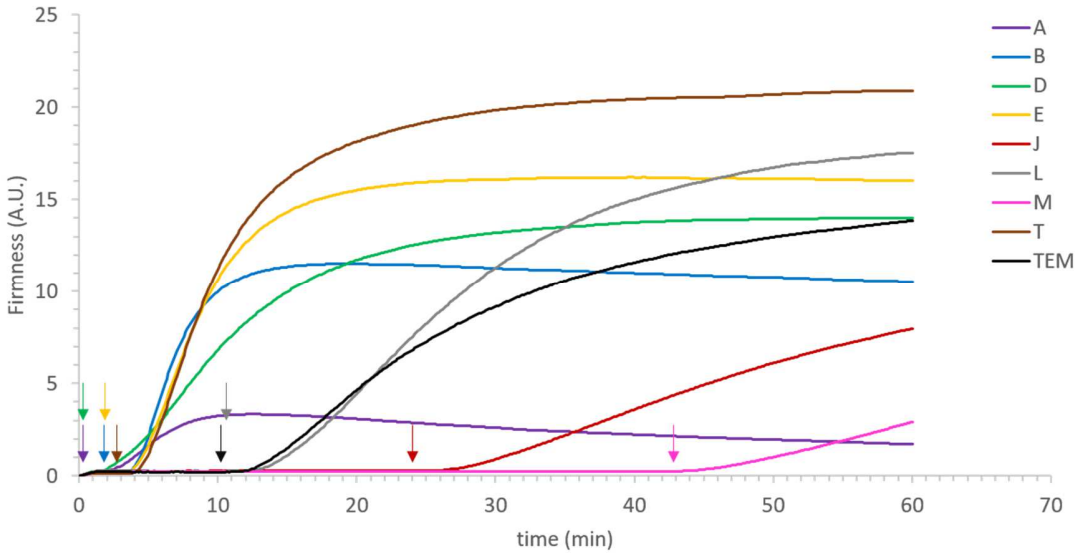

TEM
200 nm

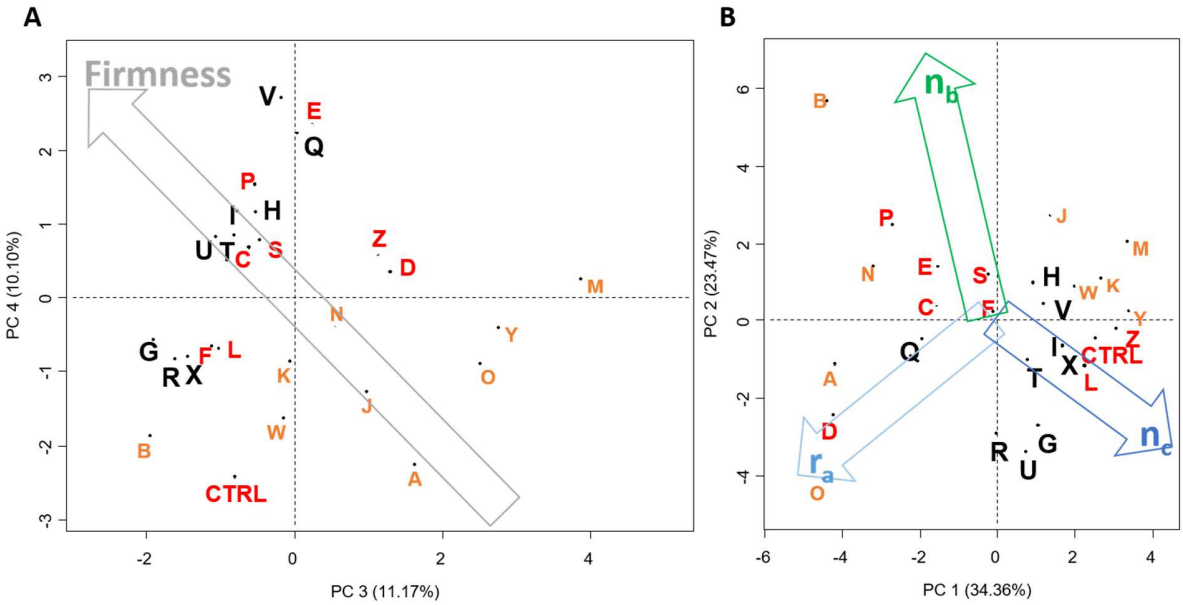
A.


Diffusible Ca
CaCl2
Diffusible Cl
Firmness
Diffusible Na
NaCl
τ
Colloidal Pi
Δρa
Diffusible Pi
nc
ra
rb
rNTA
Colloidal Ca
Colloidal Na
CT
Γs/l
nb
pH
Colloidal Cl
1.0
0.5
0.0
-0.5
-1.0
PC 4 (10.10%)
PC 2 (23.47%)

B.


V
E
Q
P
I
H
U
T
S
C
Z
D
M
Y
N
F
G
L
X
O
R
K
J
W
B
A
TEM
PC 4 (10.10%)
PC 2 (23.47%)
3
2
1
0
-1
-2
-3
-4
-2
0
2
4
6


25
20
15
10
5
0
Firmness (A.U.)
0
10
20
30
40
50
60
70
time (min)
A
B
D
E
J
L
M
T
TEM


A
Firmness
PC 4 (10.10%)
PC 3 (11.17%)
B
n_b
r_a
n_c
PC 2 (23.47%)
PC 1 (34.36%)

	Diffusible Ca (mmol kg^{-1})	Colloidal Ca (mmol kg^{-1})	Diffusible Na (mmol kg^{-1})	Colloidal Na (mmol kg^{-1})	Diffusible Cl (mmol kg^{-1})	Colloidal Cl (mmol kg^{-1})	Diffusible Pi (mmol kg^{-1})	Colloidal Pi (mmol kg^{-1})
Full experimental plan - 27 suspensions								
Average	12.4	14.8	64.8	0.2	67.4	0.5	2.4	4.6
SD	6.0	4.3	45.5	0.5	45.7	1.4	1.3	1.3
RSD (%)	48.2	29.2	70.3	300.9	67.8	287.6	55.1	28.1
minimum	2.1	3.6	6.7	0.0	0.0	0.0	0.0	1.9
maximum	22.9	20.2	135.6	2.2	138.0	6.2	5.0	7.2
Selected individual suspensions								
A	9.6	8.2	8.9	0.0	2.2	1.6	3.8	3.3
B	11.0	8.8	114.4	0.0	102.7	6.2	4.8	1.9
D	20.1	12.0	24.0	0.0	26.9	3.3	2.9	3.5
E	22.8	12.3	121.7	0.0	130.7	0.0	3.4	3.5
J	3.5	15.8	120.2	0.0	94.4	0.0	1.7	4.9
L	14.7	20.2	10.5	0.0	17.9	1.8	0.8	5.4
M	16.3	18.8	135.6	0.0	129.4	0.0	0.0	6.9
T	11.5	15.8	65.4	0.0	69.2	0.0	2.3	5.0
CTRL	2.1	18.0	6.7	0.8	0.0	0.0	1.6	4.9

	Turbidimetry	NTA	SAXS							Cryo TEM
	τ (cm^{-1})	r_{NTA} (nm)	$\Delta\rho_a$ ($e^-.A^{-3}$)	r_a (nm)	r_b (nm)	r_c (nm)	n_b	n_{cCaP}	n_{cPI}	$\Gamma_{s/l}$
Full experimental design - 27 suspensions										
Average	21.2	61.0	0.015	45.6	10.7	1.6	3.3	171.5	318.9	8.5
SD	6.8	5.5	0.002	4.2	4.2	0.0	2.8	54.0	100.4	7.8
RSD (%)	32.1	9.0	13.5	9.3	38.9	3.1	84.1	31.5	31.5	91.0
minimum	12.6	53.8	0.010	41.5	6.1	1.5	0.2	75.3	140.0	0.9
maximum	43.8	74.8	0.018	58.1	21.9	1.7	13.3	243.7	453.3	35.6
Selected individual suspensions										
A	21.4	70.8	0.011	54.7	7.6	1.7	2.1	87.0	161.9	6.7
B	14.6	53.8	0.012	45.5	6.9	1.6	13.3	75.3	140.0	35.6
D	43.8	73.4	0.012	54.5	6.1	1.6	1.6	127.4	236.9	3.0
E	18.0	59.6	0.014	46.4	7.6	1.6	4.0	121.6	226.2	6.2
J	14.0	59.3	0.016	41.8	8.7	1.6	6.6	174.2	324.0	16.8
L	13.8	59.8	0.018	43.5	12.8	1.6	1.2	231.7	431.0	6.7
M	12.6	61.8	0.017	42.3	8.3	1.6	5.1	202.6	376.9	1.7
T	24.5	62.1	0.017	44.3	12.2	1.6	1.3	203.1	377.8	6.0
CTRL	15.7	57.0	0.018	41.5	10.1	1.5	4.0	228.0	424.1	4.6

	Firmness (A.U.)	RCT (min)
full experimental design - 27 suspensions		
Average	14.9	8.6
SD	5.1	9.8
RSD (%)	34.0	113.5
minimum	3.0	1.1
maximum	20.9	42.4
Selected individual suspensions		
A	3.3	1.4
B	11.5	2.9
D	14.0	1.4
E	16.2	2.9
J	8.0	24.6
L	17.5	11.2
M	3.0	42.4
T	20.9	3.4
CTRL	13.9	11.0

Table 1: Distribution of the mineral salts in the suspensions. Colloidal concentrations were determined by subtracting the concentration of diffusible ions from the concentration of total ions. Average, standand deviation (SD), relative standard deviation (RSD), minimum and maximum values were determined on the complete set of 27 samples.

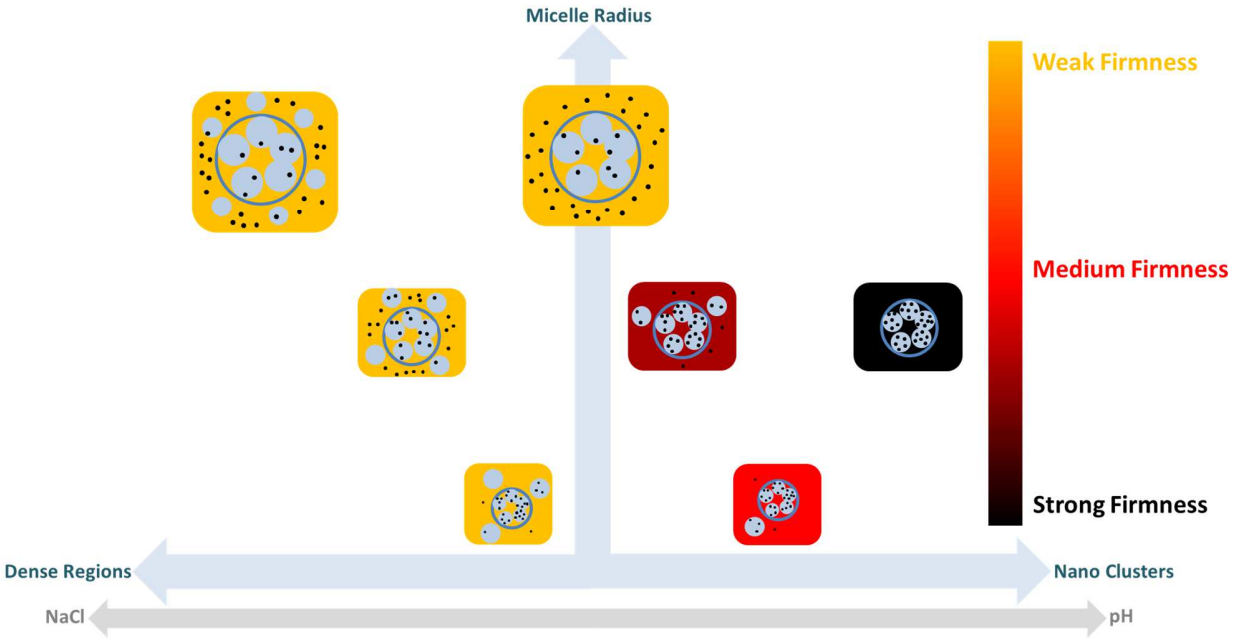
	Diffusible Ca (mmol kg^{-1})	Colloidal Ca (mmol kg^{-1})	Diffusible Na (mmol kg^{-1})	Colloidal Na (mmol kg^{-1})	Diffusible Cl (mmol kg^{-1})	Colloidal Cl (mmol kg^{-1})	Diffusible Pi (mmol kg^{-1})	Colloidal Pi (mmol kg^{-1})
Full experimental plan - 27 suspensions								
Average	12.4	14.8	64.8	0.2	67.4	0.5	2.4	4.6
SD	6.0	4.3	45.5	0.5	45.7	1.4	1.3	1.3
RSD (%)	48.2	29.2	70.3	300.9	67.8	287.6	55.1	28.1
minimum	2.1	3.6	6.7	0.0	0.0	0.0	0.0	1.9
maximum	22.9	20.2	135.6	2.2	138.0	6.2	5.0	7.2
Selected individual suspensions								
A	9.6	8.2	8.9	0.0	2.2	1.6	3.8	3.3
B	11.0	8.8	114.4	0.0	102.7	6.2	4.8	1.9
D	20.1	12.0	24.0	0.0	26.9	3.3	2.9	3.5
E	22.8	12.3	121.7	0.0	130.7	0.0	3.4	3.5
J	3.5	15.8	120.2	0.0	94.4	0.0	1.7	4.9
L	14.7	20.2	10.5	0.0	17.9	1.8	0.8	5.4
M	16.3	18.8	135.6	0.0	129.4	0.0	0.0	6.9
T	11.5	15.8	65.4	0.0	69.2	0.0	2.3	5.0
CTRL	2.1	18.0	6.7	0.8	0.0	0.0	1.6	4.9

Table 2: Size-related parameters determined by different analytical methods including Turbidimetry, NTA, SAXS and Cryo-TEM. Average, standand deviation (SD), relative standard deviation (RSD), minimum and maximum values were determined on the complete set of 27 samples. ncCaP and ncPI correspond to the number of C scatterers per casein micelle, in the case where these scatterers are considered as CaP nanoclusters or protein Inhomogeneities, respectively.

	Turbidimetry	NTA	SAXS							Cryo TEM
	τ (cm^{-1})	r_{NTA} (nm)	$\Delta\rho_a$ ($e^-.A^{-3}$)	r_a (nm)	r_b (nm)	r_c (nm)	n_b	n_{cCaP}	n_{cPI}	$\Gamma_{s/l}$
Full experimental design - 27 suspensions										
Average	21.2	61.0	0.015	45.6	10.7	1.6	3.3	171.5	318.9	8.5
SD	6.8	5.5	0.002	4.2	4.2	0.0	2.8	54.0	100.4	7.8
RSD (%)	32.1	9.0	13.5	9.3	38.9	3.1	84.1	31.5	31.5	91.0
minimum	12.6	53.8	0.010	41.5	6.1	1.5	0.2	75.3	140.0	0.9
maximum	43.8	74.8	0.018	58.1	21.9	1.7	13.3	243.7	453.3	35.6
Selected individual suspensions										
A	21.4	70.8	0.011	54.7	7.6	1.7	2.1	87.0	161.9	6.7
B	14.6	53.8	0.012	45.5	6.9	1.6	13.3	75.3	140.0	35.6
D	43.8	73.4	0.012	54.5	6.1	1.6	1.6	127.4	236.9	3.0
E	18.0	59.6	0.014	46.4	7.6	1.6	4.0	121.6	226.2	6.2
J	14.0	59.3	0.016	41.8	8.7	1.6	6.6	174.2	324.0	16.8
L	13.8	59.8	0.018	43.5	12.8	1.6	1.2	231.7	431.0	6.7
M	12.6	61.8	0.017	42.3	8.3	1.6	5.1	202.6	376.9	1.7
T	24.5	62.1	0.017	44.3	12.2	1.6	1.3	203.1	377.8	6.0
CTRL	15.7	57.0	0.018	41.5	10.1	1.5	4.0	228.0	424.1	4.6

Table 3: Rennet coagulation properties of Firmness and Rennet Coagulation Time (RCT). Average, standand deviation (SD), relative standard deviation (RSD), minimum and maximum values were determined on the complete set of 27 samples.

	Firmness (A.U.)	RCT (min)
full experimental design - 27 suspensions		
Average	14.9	8.6
SD	5.1	9.8
RSD (%)	34.0	113.5
minimum	3.0	1.1
maximum	20.9	42.4
Selected individual suspensions		
A	3.3	1.4
B	11.5	2.9
D	14.0	1.4
E	16.2	2.9
J	8.0	24.6
L	17.5	11.2
M	3.0	42.4
T	20.9	3.4
CTRL	13.9	11.0


Micelle Radius
Weak Firmness
Medium Firmness
Strong Firmness
Dense Regions
Nano Clusters
NaCl
pH